

iv)  $^{-}[^{125}\text{I}]$ sodium iodide, specific activity 15.6 mCi/ $\mu\text{g}$  (579 MBq  $^{125}\text{I}/\mu\text{g}$ ), of iodine at the activity reference date, 99.5% pure.

#### 4.8 Preparation of unilamellar and multilamellar liposomes

4.8.1 Multilamellar liposomes were prepared according to Alving et al. (1980) with slight modification by Swaney (1980). EYPC solution containing 10 mg of lipid was placed in a glass scintillator vial and the solvent removed by a low vacuum pressure, followed by treatment with a stream of gas nitrogen. The lipid was deposited onto the glass-wall as a very thin uniform film. Then 10 ml of buffer pH 7.4 (20 mM tris-HCl, 100 mM NaCl or KCl, and 0.02% (w/v) azide) was added and the vial flushed with  $\text{N}_2$  for 5 minutes. The lipid solution was dispersed using a vortex mixer for 1 minute and then sonicated (80/40 watt transistorised soniclean, Dave Instruments Ltd., London) until all the lipid was resuspended as a turbid dispersion (approximately 10 minutes at half power). This lipid suspension was centrifuged at 12,000  $g_{av}$  for 10 minutes at room temperature to remove the small liposomes left in the supernatant, and the soft pellet (containing the multilamellar liposomes) was resuspended in tris buffer<sup>e</sup> pH 7.4.

#### 4.8.2 Unilamellar liposome preparation

Vesicles or unilamellar liposomes were prepared by two different methods. In the first method, the lipid were dispersed as to multilamellar liposomes, except that the sonication was carried out at maximum power for 30 minutes. Care was taken to avoid overheating. The suspension was centrifuged at 12,000  $g_{av}$  for 10 min at 4°C and the supernatant kept. Concentrations for uni- or multilamellar liposome

suspensions / <sup>were</sup> adjusted using the phosphate method (see section 4.3.2).

A second method in order to obtain small liposomes was described by Fukushima (1981). In this method, lipid was dissolved in ethanol to 10 mg/ml and 1 ml injected into 50 ml of tris buffer pH 7.4. The suspension was concentrated to 6-8 ml by rapid ultrafiltration with a positive pressure of gas nitrogen (filter XM 300, Amicon, Lexington, Mass., USA). Particles with an equivalent molecular weight higher than  $3 \times 10^5$  are retained by this method.

The homogeneity of unilamellar liposome population was verified by chromatography in a Sepharose-4B column (60 x 1.5 cm) monitored at 325 nm as described by Huang (1969).

#### 4.9 Lipid monolayer techniques

4.9.1 Two kinds of trough were used for lipid monolayer experiments.

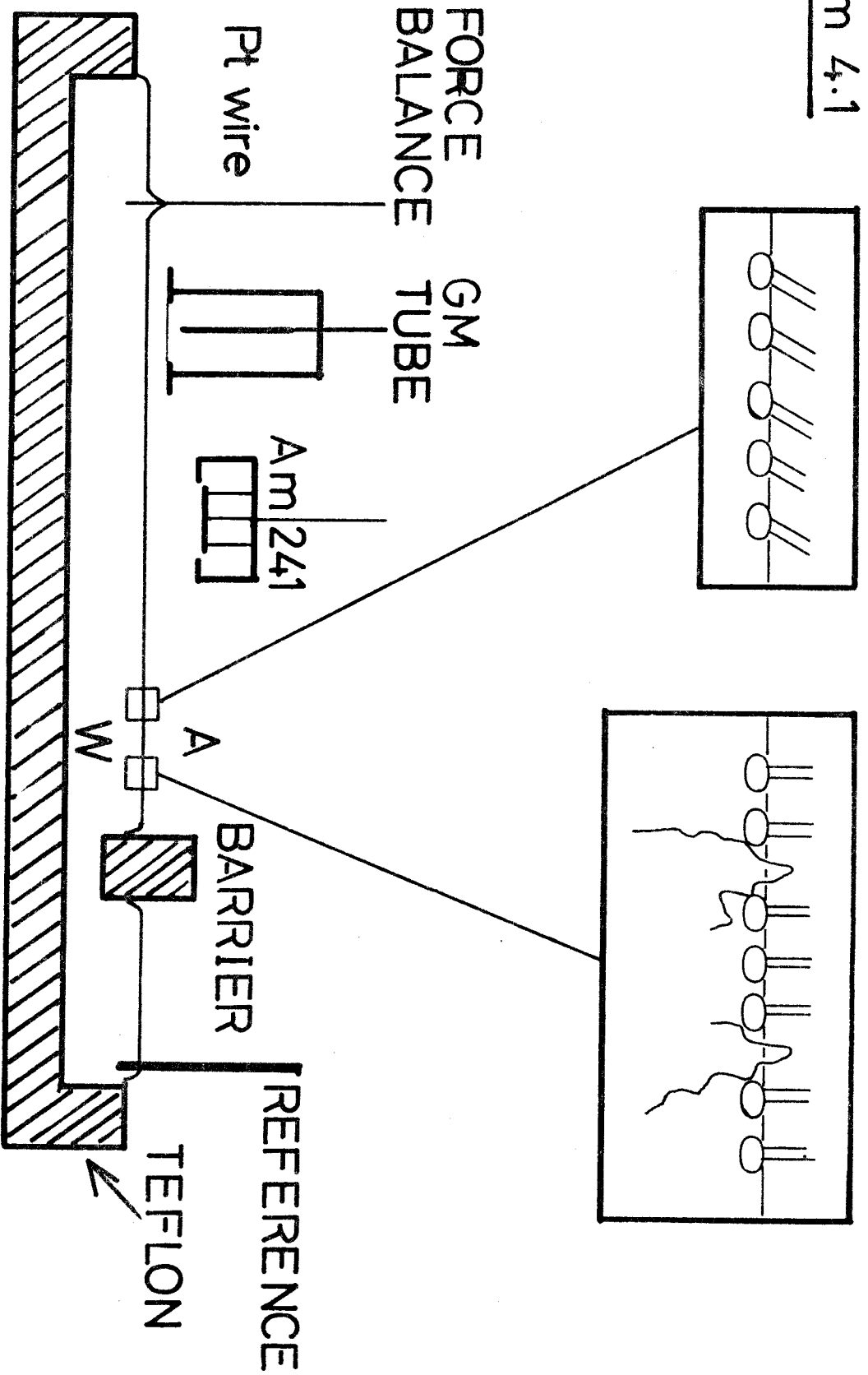
i) A Langmuir trough made from polytetrafluoroethylene (PTFE, teflon) with dimension 20 x 6 x 0.8 cm; the volume of fluid contained was 100 ml. The trough was fixed to a rigid metal base, and movable teflon barriers (0.8 x 0.8 x 7.7 cm) allowed the surface area to be varied up to a maximum of 108 cm<sup>2</sup>. An inlet drilled into one side of the trough permitted additions or withdrawals to be made from the sub-phase (also additions may be done behind the barrier) without perturbing the air-water interface.

ii) Small circular troughs were made from teflon beakers (surface area 12 cm<sup>2</sup> x depth 2 cm; volume of aqueous phase 20 ml). The circular trough was fixed to a rigid metal base, and additions and withdrawals from the subphase solution were made through an inlet drilled into one side of the trough beneath the surface (see diagrams 4.1 and 4.2).

Diagram 4.1

The large teflon trough and its various elements. Surface tension is measured using the platinum wire suspended from an electronic null-reading force balance. Surface potential due to the orientation of the film forming-molecules as dipoles, is measured using an air-ionizing electrode ( $^{241}\text{Am}$ ) with a calomel reference electrode. Surface excess radioactivity is measured using a Geiger-Muller tube connected to a ratemeter. Enlarged views of lipid monolayers alone and in presence of a protein are shown. The lipid monolayer is compressed to a convenient surface area with the teflon barrier.

Diagram 4.1



ension  
nic  
ured  
nce  
of  
a

Diagram 4.2

Schematic representation of the small circular trough showing the inlet through which additions and withdrawals from the subphase are made.

Diagram 4.3a

The water surface is cleaned by collecting a known excess of the aqueous buffer.

Diagram 4.3b

The contact angle  $\theta$  of the platinum wire with the liquid can be reduced to zero by keeping the wire surface completely wettable. (Section 4.10.1).

Diagram 4.2

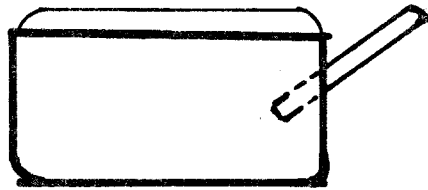


Diagram 4.3.a.

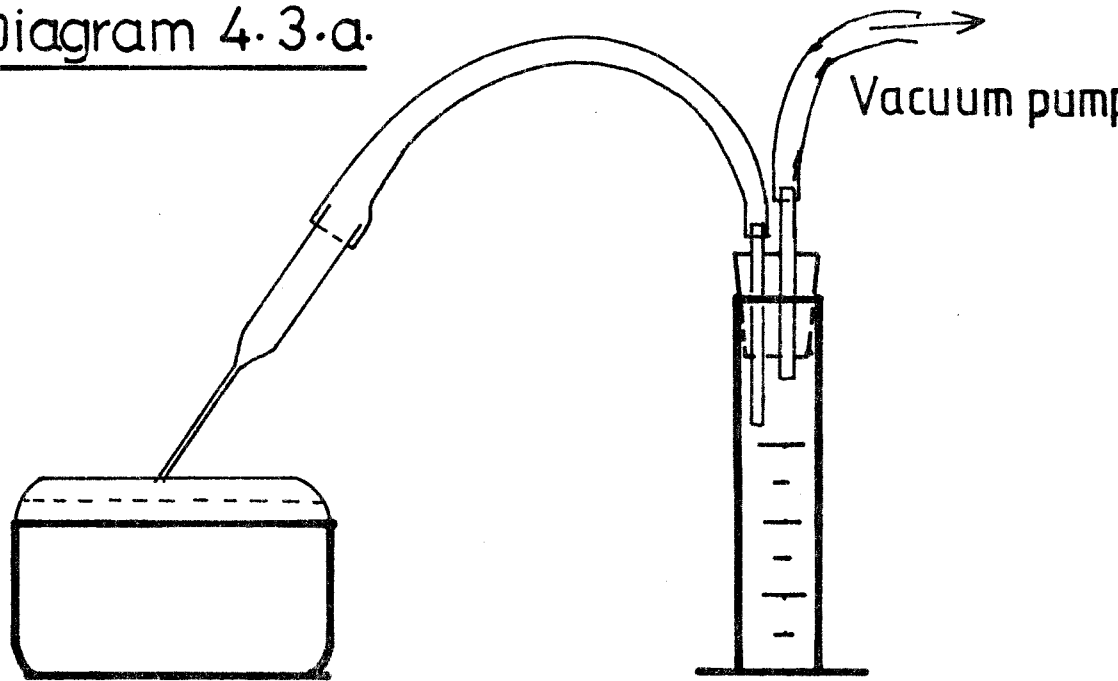
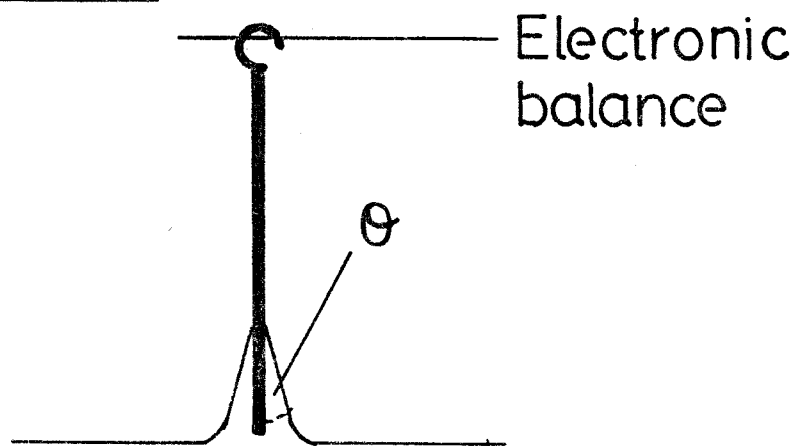


Diagram 4.3.b.



#### 4.9.2 Subphase

Unless otherwise specified, the subphase for monolayer studies consisted of 145 mM KCl, and either 10 mM Tris-HCl for experiments conducted above pH 7.0, or 10 mM Tris-maleic acid for pH's below 7.0. Buffer solutions were prepared with twice-distilled water (all glass stills after deionization through a mixed bed resin to a conductivity of better than 20 Siemens). The troughs were filled with a greater volume than required in order that the aqueous surface might be extensively cleaned. Thus, the large trough was filled with a 10 ml excess of buffer and the small circular one with approximately 4 ml excess. The excess volume was removed by aspiration using a Pasteur pipette with its tip held just at the liquid surface by a rubber pipe attached to a suction pump. The fluid was collected in a graduate receiver (diagram 4.3.a).

#### 4.9.3 Formation of lipid films

(a) Monolayers were formed in the large trough by touching the clean buffer surface with a droplet of lipid solution ( $\sim 2\mu\text{l}$ ) delivered from a Hamilton syringe. 10 seconds were allowed between each addition, and once the required amount of lipid had been added, 20 minutes were allowed to elapse in order to permit complete solvent evaporation and equilibration of the air-water interfacial film. During the time allowed for evaporation, it was found very convenient, as suggested by Phillips & Chapman (1968), to compress the film to about  $20 \text{ mN m}^{-1}$  which enhanced solvent evaporation. The stock lipid solution was kept on (0-4°C) ice/during the monolayer experiments. The film was compressed and expanded by the manually movable teflon barrier.

(b) The formation of monolayers in small circular troughs was done in a basically similar fashion, except that the droplets of lipid solution delivered to the liquid surface were approximately 0.5  $\mu$ l each. The lipid was spread on the buffer surface until the desired initial surface pressure ( $\pi_i$ ) was reached. The subphase of the trough described above was stirred in some experiments.

#### 4.9.4 The cleaning of troughs and glassware

The following procedure was applied routinely and tests using surface-pressure and surface potential measurements showed no contamination by surfactive agents. A bio-degradable detergent RBS (Chemical Concentrates (RBS) Ltd, London) diluted to 5% (v/v) with hot tap-water was used to wash troughs and glass ware. It was removed by (a) rinsing the troughs with hot tap-water, (b) soaking them in 50% nitric acid for at least 30 min, rinse again with hot tap-water and (c) rinsing again with distilled water for at least 2 hours.

#### 4.10 Measurements of monolayer properties

##### 4.10.1 Surface pressure

Surface pressure was determined using a modified Wilhelmy dipping plate technique (Rothfield & Fried, 1975). A thin platinum wire (diameter 0.0508 cm) was suspended from an electronic balance (C.I. Electronics Ltd., Salisbury, U.K.) so that it touched and just penetrated the monolayer, with optical servo-control of beam position and thus automatic compensation for the buoyancy correction of the immersed portion of the wire (Davies & Rideal, 1963). The surface of the platinum wire was kept clean and rough before each experiment by either flaming until it turned red or immersing in 4 M HCl for 2 minutes. These processes, make the treated wire portion completely wettable so that  $\theta$ , the contact angle, will approach zero (diagram 4.3.b). Surface pressure was calculated using equation (3.3). The buoyancy factor was



taken as zero since it is corrected automatically by the electrical balance.

#### 4.10.2 Surface potential

Surface potential was measured with a model 602 electrometer (Keithley Instruments Inc., Cleveland, Ohio, USA) connected to an air-ionizing electrode of Americium 241 suspended 5-8 mm from the air-water interface and to a calomel reference electrode immersed in the subphase behind one of the teflon barriers. The air-ionizing electrode of 241 Am was designed and built by Dr R.A. Klein in this laboratory, and provides a surface area of  $0.636 \text{ cm}^2$ . The electrode was of a special concentric guard-ring construction, and was extremely stable in use with minimal screening, particularly against interference from 'stray' capacitance or electrostatic fields produced by nearby hands or arms. The surface potential produced by the orientation of the surface dipoles was measured using a high input-impedance ( $\sim 10^{14}$  ohms) electrometer much greater than the gap resistance ( $\sim 10^{10}$  ohms) (see diagram 4.4).

#### 4.10.3 Surface adsorption of radiochemicals

Measurements of radioactive material adsorbed to the surface film were carried out by two different methods.

i) A direct method in which radioactivity was estimated using a thin end-window Geiger-Muller tube, with a counting efficiency of  $\sim 6\%$  for  $^{14}\text{C}(\beta)$ . This tube was held approximately 8 mm above the lipid film and connected to a ratemeter (P7900A, Panax Equipment Ltd., Surrey, England). A counting time of 10 min was used together with a long time constant ( $\tau = 30$  sec). The method relies for both its sensitivity and lack of subphase interference, such as backscattering of  $\beta$  particles

Diagram 4.4

Simplified block diagram, modified to show the guard connection, taken from the Keithley Model 602 Manual. A full circuit diagram of the instrument is also shown (Diagram 4.4, appendix).

Lo : low circuit

Hi : high circuit

A : amplifier

Q1 and Q2 are transistors

S to fix the voltage range

M : meter

F : feedback switch

E : potentiometer

Air-Ionizing  
electrode

Reference  
electrode

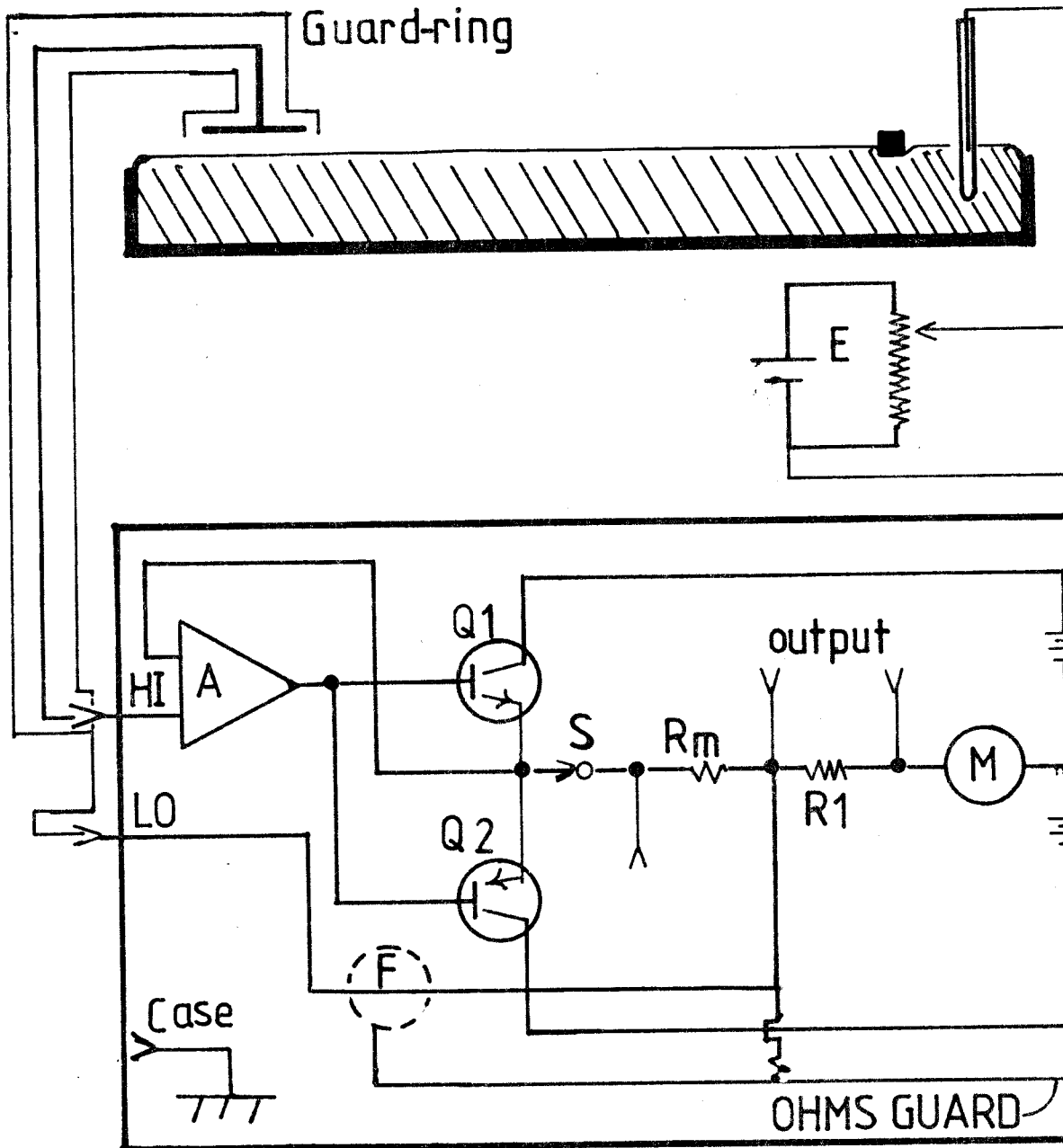


Diagram 4.4

(Gaines, 1960), on the limited range of emitted particles in water (Davies & Rideal, 1963). Ranges for the  $\beta$ -radiation emitted by  $^3\text{H}$  (0.018 MeV) and  $^{14}\text{C}$  (0.155 MeV) of 6  $\mu\text{m}$  and 300  $\mu\text{m}$  respectively have been reported by Aniansson (1951) and Gershfeld (1974).  $^{125}\text{I}$  emits  $\beta$  (0.61 MeV) and  $\gamma$  (0.36 MeV) particles with an apparent range in water of 300  $\mu\text{m}$  and 2 mm respectively. These energies in conjunction with some properties (e.g. non-specific adsorption) of the  $^{125}\text{I}$  labelled molecule produced experimental difficulties in the measurement of the surface radioactivity.

(i) An indirect method. An attempt was made to collect the monolayer from the liquid surface and measure associated radioactivity directly in a gamma counter. Briefly, following Rietsch et al. (1977), a plastic container of 5 ml designed for radioimmunoassay was modified as follows. A thin capillary was bent in such a way that one part was inserted through the top cap, and the other tip could touch the liquid surface at a slight inclination. A 21 G needle was passed through the same tube cap and linked via a rubber pipe to a vacuum pump (diagram 4). With the capillary making  $\sim 30^\circ$  to the monolayer plane and the tip inserted in the liquid meniscus, the film was slowly compressed and fluid aspirated simultaneously from the meniscus until a volume of 5 ml was collected. Finally, the glass capillary was cut in pieces and placed into the plastic container. After sealing the container the sample radioactivity was measured directly in the gamma counter. After monolayer collection, the procedure was repeated on the same subphase with another container to determine the background counts.

#### 4.10.4 Recording conditions

The output signals from micro-force balance, ratemeter and electro-

meter were connected to a multi-channel recorder (Speedomax G, Leeds & Northrup Co., Birmingham). Thus, surface pressure, surface potential and excess surface radioactivity could be recorded concurrently and independently against time. The trough and its components were enclosed in a Faraday cage box to provide electrostatic screening.

Before spreading the film the subphase was checked for absence of surfactive agents originating from the solvents by measuring the change in surface pressure and surface potential that occurred on compression to 40% of its initial surface area. These changes amounted to less than  $\pm 0.6 \text{ mN m}^{-1}$ , or  $\pm 5 \text{ mV}$ , for the subphase alone. This method was also used to check for the absence of impurities in solvents after spreading and evaporation from the surface.

The values reported here for the force-area curves ( $\pi$ -A curves) are averages of duplicate or triplicate measurements. Reproducibility of different  $\pi$ -A curves for the same monolayer was within  $\pm 2 \text{ \AA}^2$  on the x-axis, within  $\pm 1 \text{ mN m}^{-1}$  on the Y-axis, and within  $\pm 10 \text{ mV}$  for measurements of surface potential.

#### 4.11 Gel filtration experiments

Column chromatography was performed using Sephadex G-25, G-50, LH-20 (Pharmacia Fine Chemicals, Inc., Uppsala, Sweden) and Biogel P-6 (Bio-Rad Laboratories, Richmond, CA, USA). Gels were equilibrated first with Tris-HCl buffer pH 7.2 (25 mM Tris-HCl, 50 mM KCl, 3 mM  $\text{Na}_2\text{S}_2\text{O}_3$ ), except for Sephadex LH-20 which was equilibrated with Tris-HCl buffer pH 7.2:methanol 4:1 (v/v). Column dimensions were 12 x 0.6 cm (Hummel & Dryer, 1962).

##### 4.11.1 Radioactive buffer

100  $\mu\text{Ci}$  [ $^3\text{H}$ ]cholesterol was placed in a

glass vial with a final volume of 4-5 ml in chloroform. The solvent was removed by means of reduced pressure, and the expanded thin film remaining on the wall of the glass vial treated with a stream of gas nitrogen. 5 ml Tris-HCl buffer pH 7.2 was added and vortexed until the film had been dispersed; 50  $\mu$ l aliquots were added to 5 ml of Packard scintillation cocktail (Scintillator 299) and radioactivity determined using a Packard model 460 CD Tri-Carb liquid scintillation counter. The radioactive solution was adjusted to / desired radio-activity, ie. 234,000 cpm/ml and will now be referred to as radioactive buffer (RB).

The column was equilibrated with RB as follows: after passing a volume of twice the void volume ( $\sim$  2 ml) fractions of RB (0.25 ml) were collected and radioactivity measured. When a constant level of radioactivity was attained in each fraction this was taken to indicate the column had reached equilibrium. The antigen was incubated with 0.25 ml RB and applied to the column. Eluant was collected in 0.25 ml fractions and monitored at 280 nm to locate any protein peak. Radio-activity was measured in 50  $\mu$ l of each fraction as described above. The disintegrations/min/sample were computed using the sample channels ratio method (Cooper, Chapter 3, 1977) and a series of quenched standards of known [ $^3$ H] content (Packard Inst. 295,000 dpm  $\pm$  1.4%). These calculations were performed by the microprocessor contained within the scintillation counter.

#### 4.12 Polyene antibiotics

Filipin was a gift from Dr G. Whitfield, Upjohn Company, Kalamazoo, Michigan, U.S.A. Filipin was made up at a concentration of 1 mM in dimethyl formamide. Amphotericin B was kindly provided by Dr D. Kerridge,

Department of Biochemistry, University of Cambridge. Amphotericin B was prepared at a concentration of 1 mM in dimethyl sulfoxide.

Antibiotic solutions were freshly prepared and used within a maximum period of 3 days.

#### 4.13 Temperature programming method

Multilamellar liposomes of DPPC/DMPC, DPPC/DMPC/cholesterol or DMPC/cholesterol were prepared as described in Section 4.8, and the lipid composition for each is given in the section of results. 0.8 ml of a multilamellar liposome suspension with an average of 0.2 mg per ml were added into a thermostated spectrophotometer cell and equilibrated at 10°C for 10 minutes. This cell was heated electrically using an electronic temperature programmer (SP 876, Temperature Programme Controller Accuron Ltd, Cambridge, England). The temperature was raised linearly from 10 to 40°C at a rate of 0.5°C per minute according to Pownall *et al.* (1978) and Swaney & Chang (1980). The increase of the temperature and the absorbance (325 nm) were recorded continuously through the heating rate. The cells were cooled by passing water through pipes connected to the cell-holder. VSG and liposomes at the desired concentration (shown in results), were mixed in the cuvette and the procedure was as above.

#### 4.14 Centrifugation of liposome-VSG mixture in sucrose gradient

Unilamellar liposomes were prepared after a lipid dispersion was ultrasonically irradiated (Section 4.8) and the concentration of phosphatidyl choline was adjusted by measuring the phosphate content (Section 4.8). A volume of 0.25 ml of liposome suspension was incubated with 0.5 mg of VSG for a final volume of 0.35 ml (0.1 M KCl, 0.01 M Tris-HCl, 0.001 M azide, pH 7.2), and a mol ratio of phospholipid to VSG of 24:1.

9

Various mol ratios of phospholipid to cholesterol were used as shown in results. The incubation of this liposome-VSG mixture was carried out at room temperature with continuous mechanical mixing on a rotating wheel for 16 hours. At the end of this incubation the samples were added to the top of a sucrose gradient (4.6 ml, 16% to 46% w/v) in 5 ml nitrocellulose tubes and centrifuged at  $170,000 g_{av}$  for 20 hours at  $5^{\circ}C$  (Ultracentrifuge L2-65B, Beckman Instruments).

The gradient was monitored at 280 nm and collected in 0.5 ml fractions (Isco density gradient fractionator, Model 185, Instrumentation Specialities Co., Nebraska, U.S.A.). The refractive index of each sample was determined at  $25^{\circ}C$  using a refractometer (Bellingham & Stanley Ltd, U.K.). The corresponding percentage of sucrose (w/v) is expressed as the gradient profiles.



CHAPTER 5

RESULTS

RESULTS5.1 Properties of phospholipid monolayers and their interaction with VSG

Phospholipid monolayers show  $\pi$ -A/ $\Delta V$  - A curves from which information about the physical state of their film-forming molecules can be evaluated. Compression of the film at temperatures above or below the lipid transition produces an expanded or a condensed film respectively, as well as a different surface packing (surface area per molecule,  $\text{\AA}^2/\text{molecule}$ ) for the same lipid class (Phillips & Chapman, 1968)

Studies of the VSG-phospholipid interaction have been carried out using two different approaches: (i) studying the compressibility of VSG incorporated into the lipid film and (ii) studying the penetration by molecules of VSG of a performed monolayer at constant surface area and a known initial surface pressure (see section 5.4).

5.1.1 Phosphatidyl choline (EYPC) has been shown by Williams & Chapman (19) to have a transition temperature of  $-15$  to  $-7^\circ\text{C}$  when cooled or heated respectively. A characteristic  $\pi$  - A isotherm for EYPC spread at the air-water interface is shown in Figure 5a. At room temperature this monolayer exhibits a fully expanded force area curve with a gradual increase in surface pressure when the area per molecule is reduced from values below  $120 \text{\AA}^2$ . The increase in surface pressure and surface potential attained higher values as the reduction in area per molecule reached the limiting area. Thus, for the EYPC monolayer, these values were  $60 \text{\AA}^2$  for the limiting area when the surface pressure was

increased to  $36 \text{ mN.m}^{-1}$  and a corresponding surface potential of  $480 \pm 5 \text{ mV}$ . These values are very similar to those reported in the literature for the EYPC collapse point (Phillips *et al.*, 1972 ; Demel *et al.*, 1972; Barenholz & Thompson, 1980).

Values of surface pressure and surface potential higher than these values led to the loss of some molecules from the film as deduced from a downward displacement of the  $\pi - A$  and  $\Delta V - A$  curves when the film was compressed a second time. It was important to measure the  $\pi - A$  curves and  $\Delta V - A$  curves in order to verify other properties of the lipid film. The time required to obtain a complete  $\pi - A$  curve was approximately 30 - 40 minutes; care was taken to avoid the formation of any surface pressure gradient by compressing the film slowly (Gaines, 1966, p. 144).

#### 5.1.1.1 Interaction with VSG

A phosphatidyl choline (EYPC) monolayer was formed at the air-water interface and its stability was checked by compressing and recording  $\pi - A$  curves and  $\Delta V - A$  curves. This procedure removed any retained solvent within the lipid phase (Phillips, 1968). Care was taken, however, not to reach values of surface pressure too close to the collapse pressure. The antigen used in this experiment was VSG<sub>151</sub> (MIT at 1.6) and the subphase (10 mM Tris-Maleic acid or Tris-maleate, 145 mM KCl) was adjusted to pH 6.8, the isoelectric point of this VSG. VSG<sub>151</sub> was added to the preformed EYPC monolayer at  $110 \text{ \AA}^2$ /molecule of lipid. Two ways of adding antigen were assessed; first by injecting the antigen beneath the lipid film, and second by touching the lipid surface with successive droplets of VSG solution until the desired amount had been added. Surface pressure and surface potential

reached an equilibrium in 40 minutes using the second method compared with 90 minutes for the first method. The second method, however, was found to be more favourable for studying the compressibility of VSG because of the short time needed to attain equilibrium, whilst the first one was more suitable for penetration experiments. In both methods the equilibrium was defined as the time taken until no further changes in surface pressure and surface potential could be observed. After equilibrium was attained, the mixed monolayer was compressed slowly and a new equilibrium attained for each point observed. In general it took about five minutes to reach new stable values.

The displacement of  $\pi - A$  and  $\Delta V - A$  curves for EYPC due to the presence of VSG is shown in Figure 5a.

$$\pi_{L-VSG} - \pi_L = \Delta\pi_{VSG} \quad \dots\dots\dots (5.1)$$

if the  $\pi - A$  curve for phospholipid - VSG was subtracted from the  $\pi - A$  curve for phospholipid alone at the same area per molecule of lipid, then an increment in surface pressure was obtained which could be regarded as the value due to the molecule of VSG inserted in the lipid monolayer. The change in surface pressure due to VSG ( $\Delta\pi_{VSG}$ ) remained constant for larger values of total surface pressure, see Figure 5.14(a), but at  $15 \text{ mN.m}^{-1}$  it started to diminish gradually. From these  $\pi - A$  isotherms it is possible to calculate the lateral compressibility coefficient ( $\delta$ ) as discussed later in this Chapter.

Changes in the surface potential of EYPC monolayers in the presence of VSG are also shown in Figures 5.1(a) and 5.1(b). The  $\Delta V - A$  curves for EYPC - VSG monolayers show a slight increase in  $\Delta V$  values in comparison with  $\Delta V - A$  isotherms for EYPC alone. This property

Fig. 5.1a

Egg yolk phosphatidyl choline monolayers spread at the air-water interface, 0 surface pressure and  $\bullet$  surface potential. 4 nmol of VSG<sub>151</sub> was added beneath a EYPC (18 nmol) monolayer and  $\Delta$  surface pressure and  $\blacktriangle$  surface potential determined. The subphase composition was 10 mM Tris, 145 mM KCl, pH 6.8. Room temperature:  $21 \pm 2^\circ\text{C}$

Fig. 5.1b

Effect of various concentrations of VSG in EYPC monolayers. To a preformed EYPC (18 nmol) monolayers, various concentrations of VSG were added as follows: 4 nmol,  $\blacksquare$  surface pressure and  $\square$  surface potential; 8 nmol,  $\circ$  surface pressure and surface potential; 12 nmol,  $\Delta$  surface pressure and surface potential; and 18 nmol of VSG,  $\times$  surface pressure and surface potential. The subphase was as in (a).

FIG. 5.1.a.

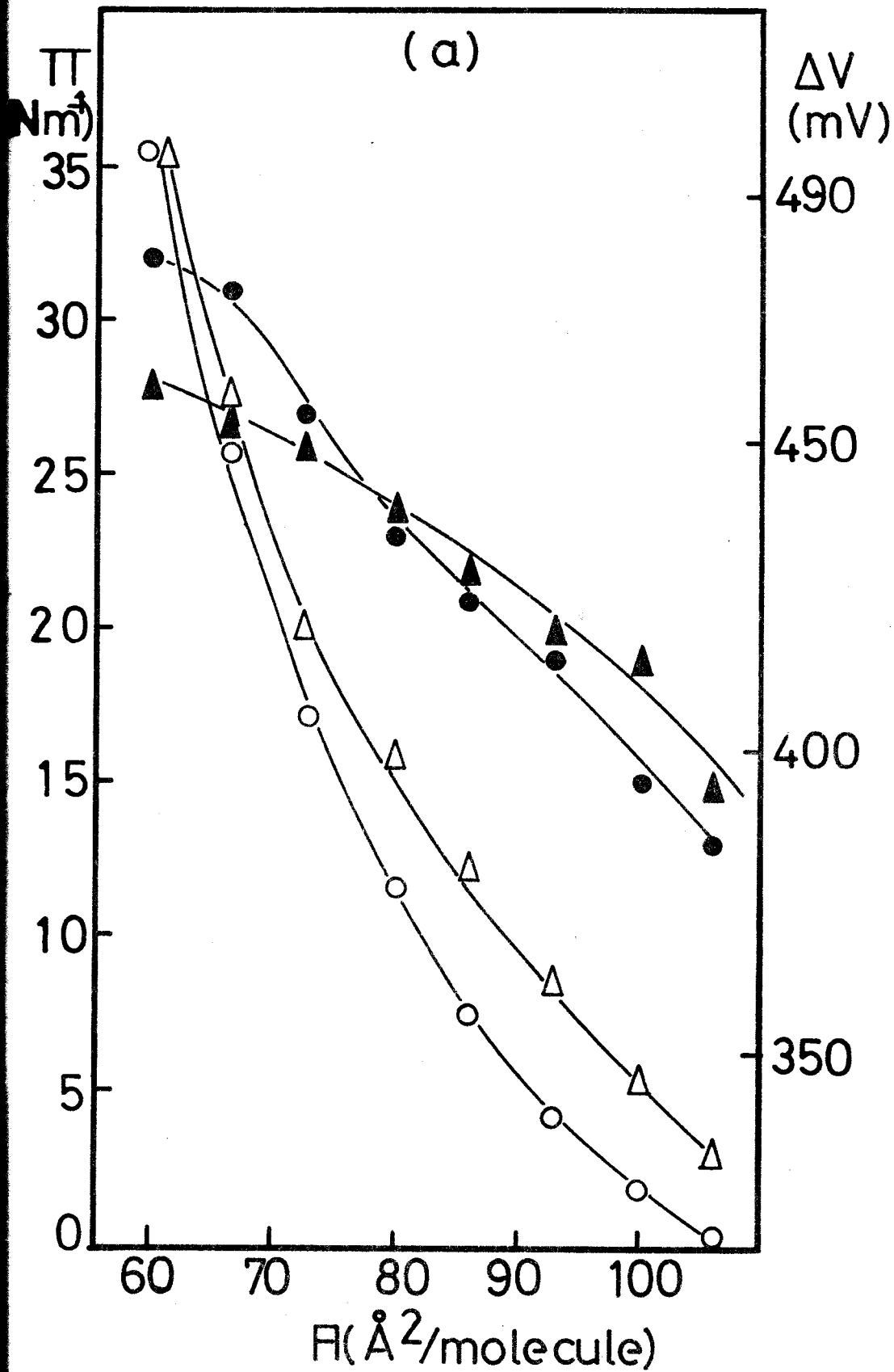
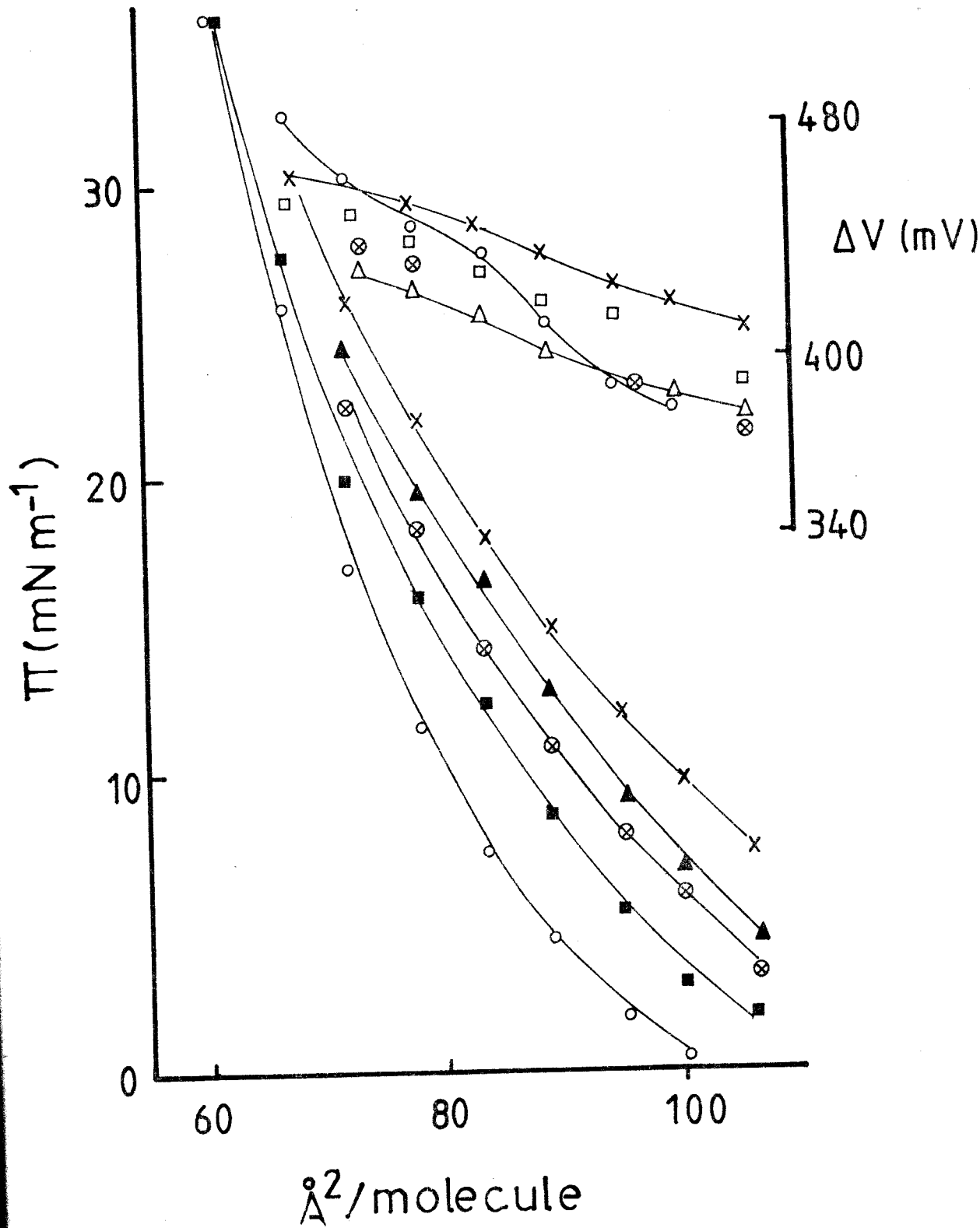


Fig. 5.1.b.



was also observed with other phospholipids, i.e., DOPC (Figure 5.3) or PE (Figure 5.6).

#### 5.1.1.2 Effect of VSG concentration

The  $\pi$  - A curves for EYPC - VSG were displaced from their original values as the VSG concentration was increased. This effect was only seen for  $\Delta V$  - A curves when the EYPC-VSG molar ratio was 1:1 as shown in Figure 5.1(b). The positive displacement of the  $\pi$  - A curves was dependent on VSG concentration, suggesting that there was not saturation of the available lipid surface area. The  $\Delta\pi_{VSG}$ , however, was not large enough as to support the interpretation of a significant insertion of molecules of VSG in the lipid film except when larger quantities of VSG were added, i.e., the EYPC : VSG molar ratio 1:1 (VSG concentration 11  $\mu\text{g/mL}$ ).

#### 5.1.2 Soybean phosphatidyl choline monolayer

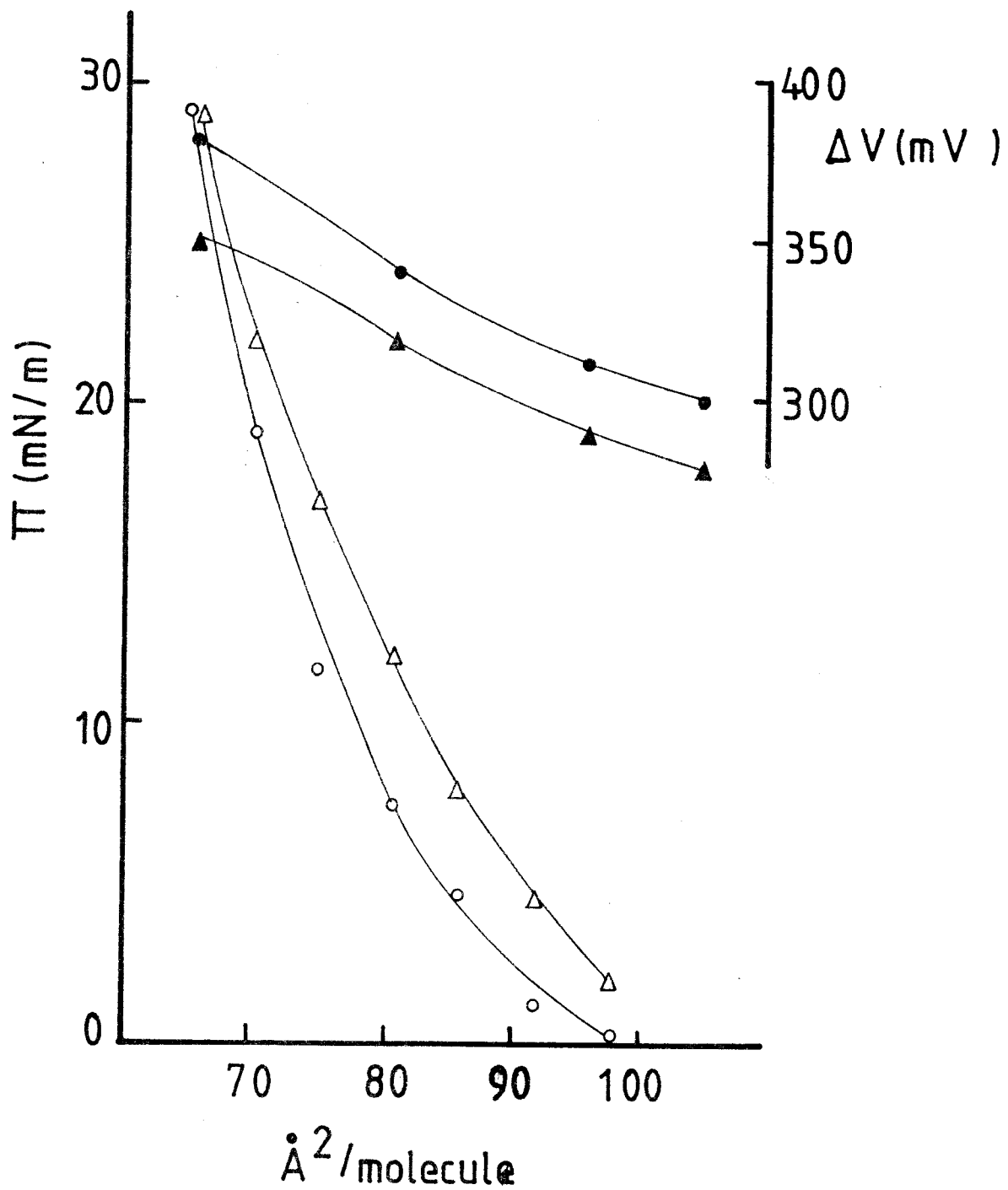
Soybean lecithin has been reported to have a large proportion of linoleic acid (C 18:2) and other unsaturated fatty acids, C 18:2 comprising approximately 70 mole % (Klein, 1972 ; Gould, 1982). Also it is known that the presence of double bonds confers more fluidity and the monolayer becomes more expanded due to the reduction of transition temperature. A soybean phosphatidyl choline (SPC) monolayer formed at the air-water interface, was allowed to interact with VSG [5] using the same experimental conditions described for EYPC-VSG. The  $\pi$  - A curve (Figure 5.2) shows a similar profile to those shown for the EYPC-VSG interaction.  $\Delta V$  - A curves show a reduction of about 10 mV in presence of VSG, which increases as the area per molecule of lipid is reduced. This suggests that increasing the percentage of unsaturated fatty acids in phosphatidyl choline is not a pre-requisite for improving



Fig. 5.2

Soybean phosphatidyl choline monolayer (17 nmoles), 0 surface pressure and ● surface potential. In presence of 4 nmoles of VSG, Δ surface pressure and ▲ surface potential. Subphase as described in Fig. 5.1a.

Fig. 5.2



the PC-VSG interaction.

### 5.1.3 Dioleoyl phosphatidyl choline monolayers

1-palmitoyl-2-oleyl lecithin is the major component (70 mole %) of egg yolk lecithin and most biological membranes (Ladbroke & Chapman, 1969); the behaviour at the air-water interface of mixtures of fatty acids contained in different lecithins, i.e., distearoyl/dioleoyl lecithin is essentially the same as for 1-stearoyl-2-oleoyl lecithin, however, their transition temperatures differ significantly (Phillips *et al.*, 1972; McElhaney, 1982).

Dioleoyl phosphatidyl choline (DOPC) a synthetic lecithin containing only one type of nonsaturated fatty acid (C 18:1), was used to study whether the interaction with VSG could be enhanced, reduced or remained the same as for EYPC monolayers. The results are shown in Figure 5.3; the isotherm curves for  $\pi - A$  and  $\Delta V - A$  are shown in the presence and absence of VSG. In comparison with EYPC monolayers, DOPC is more expanded with lower values of  $\Delta V$ . In presence of VSG at a similar concentration the displacement of both isotherms ( $\pi - A$  and  $\Delta V - A$ ) does not differ significantly from those observed for EYPC - VSG.

The present results suggest that the presence of unsaturated fatty acids other than oleic acid in phosphatidyl choline, does not produce significant changes in the PC - VSG interaction.

### 5.1.4 Dimyristoyl phosphatidyl choline

Dimyristoyl phosphatidyl choline (DMPC) monolayers were formed at the air-water interface under experimental conditions similar to those described for EYPC. The plot of  $\pi$  versus area (A) is shown in Figure 5.4; the shape of the  $\pi - A$  curve correspond to that of an

Fig. 5.3

Dioleoyl phosphatidyl choline monolayer (14 nmoles), 0 surface pressure and ● surface potential. In presence of 4 nmoles of VSG, Δ surface pressure and ▲ surface potential. Subphase as in Fig. 5.1a.

Fig. 5.3

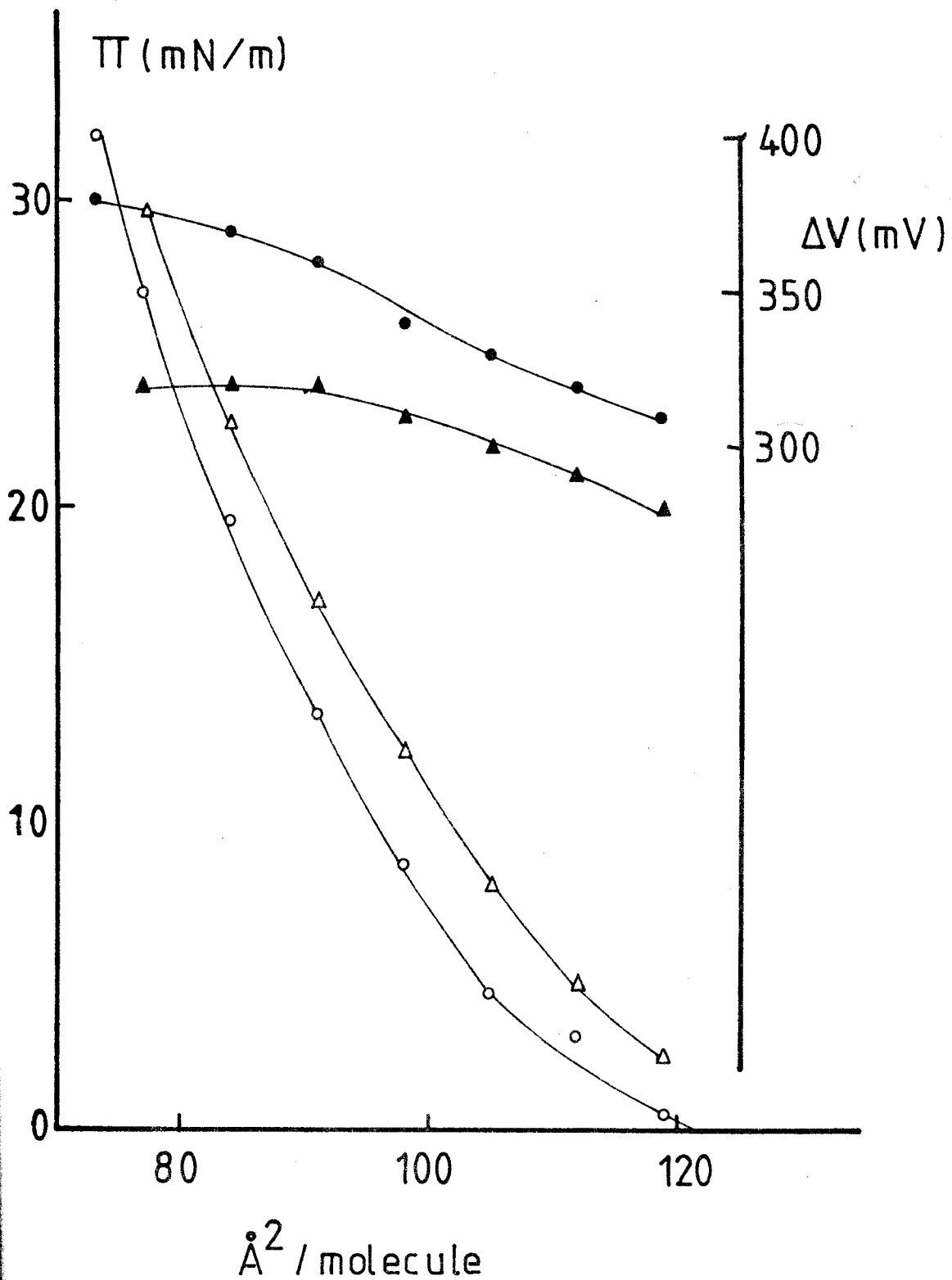
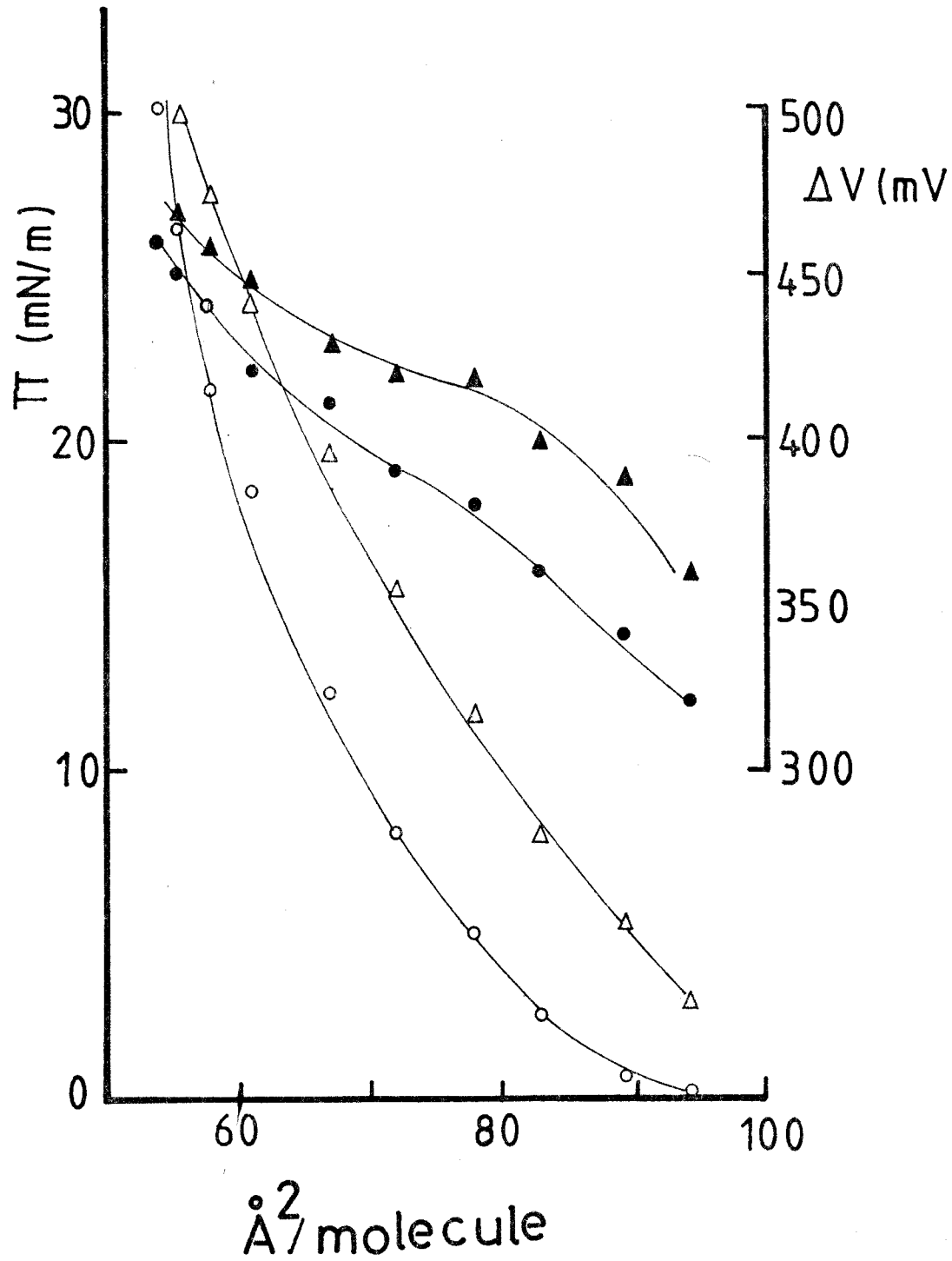


Fig. 5.4

Dimyristoyl phosphatidyl choline monolayer (18 nmoles), 0 surface pressure and ● surface potential. After adding 3 nmoles of VSG, Δ surface pressure and ▲ surface potential. Subphase pH 6.8.

Fig 5.4



expanded film, but with less compressibility than that shown by PE and EYPC monolayers. This could be due to the experimental temperature being  $2^{\circ}\text{C}$  below its transition temperature ( $T_c$ )  $23.9^{\circ}\text{C}$ ; it is known that in this condition DMPC is in a mesomorphic state (Williams & Chapman, 1972; Phillips, 1972; Swaney, 1980).

The  $\Delta V$  increases as the area per molecule decreases, and reaches higher values (about  $480 \pm 10$  mV) close to the minimum area; similar results have been reported by Colacicco & Basu (1978). The addition of VSG to the preformed monolayer produced a positive displacement of both  $\pi - A$  and  $\Delta V - A$  curves, which resemble those observed for the other phospholipids.

#### 5.1.5 Dipalmitoyl phosphatidyl choline

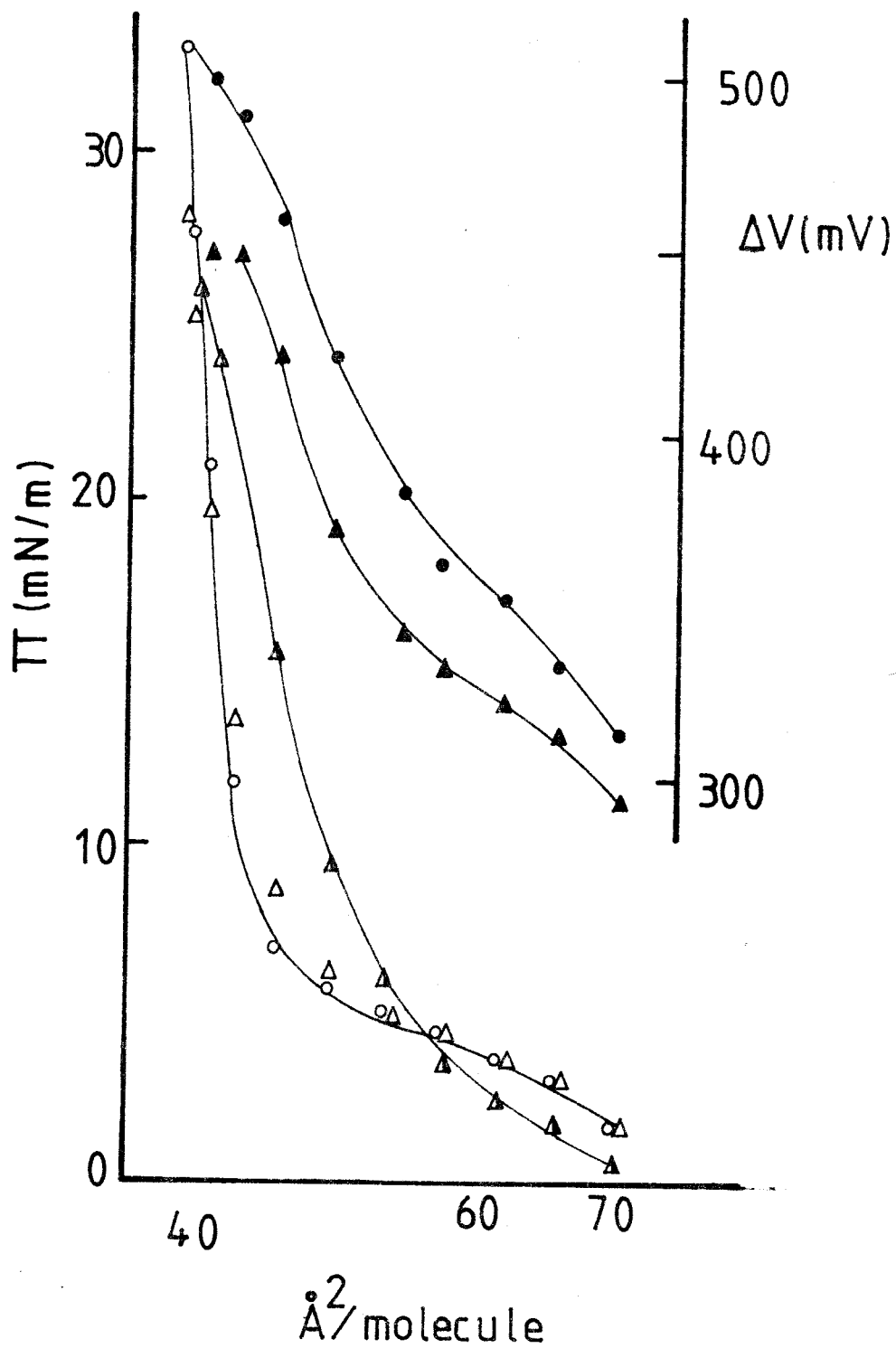
Dipalmitoyl phosphatidyl choline (DPPC) monolayers were formed at the air-water interface as described for EYPC. The force area curve of DPPC looks rather different from that observed for the other phospholipids: EYPC, SPC, DOPC, DMPC and PE. The  $\pi - A$  curve clearly shows two slopes; one which corresponds to a condensed phase between 40 and  $50 \text{ \AA}^2$ , and a second, between 50 and  $70 \text{ \AA}^2$  corresponding to an intermediate state. Phillips & Chapman (1968) has suggested that below the transition temperature for DPPC ( $41^{\circ}\text{C}$ ) the film, which is in the intermediate state, consists of crystalline cluster of molecules that are immiscible with the bulk phase which exhibit a cooperative transition. This latter has been confirmed with the more detailed studies of X-ray diffraction and differential scanning calorimetry (Tardieu et al., 1973; Chen et al., 1980; Ruocco & Shipley, 1982). The phase transition is highly sensitive to changes in temperature which in fact lead to a variety of type  $\pi - A$  isotherms for phospholipids (Phillips & Chapman, 1968; and fatty acids (Baret, 1982).



Fig. 5.5

Dipalmitoyl phosphatidyl choline monolayer (24 nmoles), spread at the air-water interface, 0 surface pressure and 0 surface potential. After adding 2 nmoles of VSG no changes in ( $\Delta$ ) surface pressure were observed, for 4 nmoles of VSG. Changes in  $\Delta$  surface pressure and  $\Delta$  surface potential were measured and are shown.

Fig.5.5



The  $\pi - A$  and  $\Delta V - A$  curves for DPPC monolayers shown in Figure 5.5 are very similar to those described in the literature (Phillips, 1972). Changes in  $\Delta V$  rise sharply to values of  $500 \pm 10$  mV near to the minimum area in good agreement with data reported by Colacicco & Basu (1978). The addition of VSG 151 to a stable DPPC monolayer did not show substantial changes in surface pressure compared with other phospholipids. Furthermore, changes in surface potential were less than those of DPPC alone.

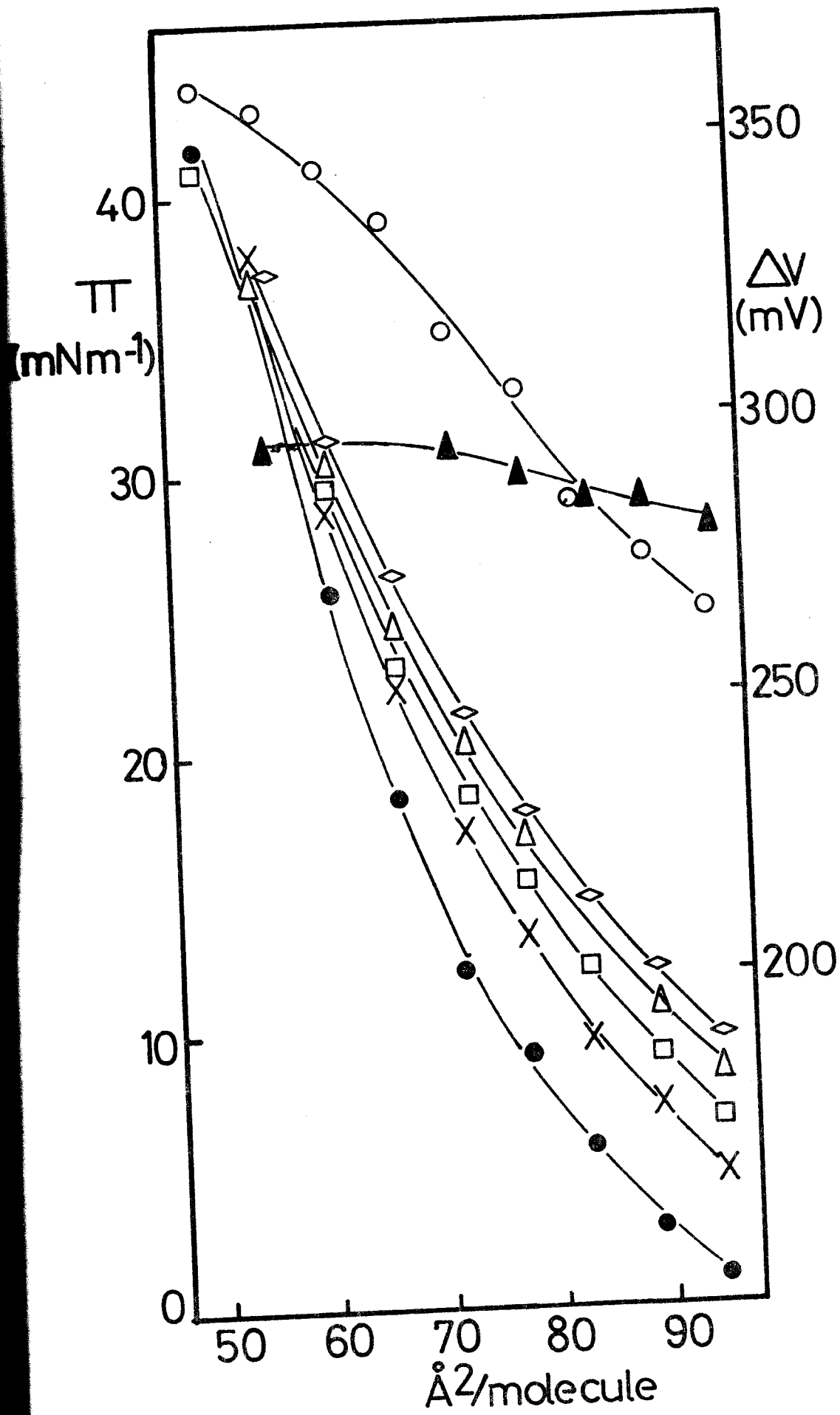
#### 5.1.6 Phosphatidyl ethanolamine

Egg yolk phosphatidyl ethanolamine (PE) formed expanded monolayers at the air-water interface; it appeared to be less expanded than phosphatidyl choline. The explanation given for such behaviour arises from steric factors associated with the large polar groups of PC and PE. The larger limiting area found for PC compared with that for PE reflects the greater space required by the bigger, and probably more hydrated, choline groups (Williams & Chapman, 1972; Hauser & Phillips, 1979). The surface potential-area curves, however, show lower  $\Delta V$  values near to the limiting area of PE than those found for PC alone; at minimum area of  $50 \text{ \AA}^2/\text{molecule}$  PE exhibited a value of about 360 mV which is lower than reported for synthetic PE (Phillips & Chapman, 1968).

Phosphatidyl ethanolamine was spread at the air-water interface under similar conditions described for EYPC. After recording the isotherms ( $\pi - A$  and  $\Delta V - A$ ) by compressing to below the collapse pressure VSG was added by touching the lipid surface at  $95 \text{ \AA}^2$  ( $\sim 2$  mN/m). After 40 minutes the lipid film was compressed again and the  $\pi - A$  and  $\Delta V - A$  isotherms recorded. The  $\pi - A$  curve for PE (Figure 5.6) resembles that for the VSG-EYPC interaction (Figure 5.1b), except that only a  $\Delta V - A$  curve is shown for clarity.

Fig. 5.6

Phosphatidyl ethanolamine monolayer spread at the air-water interface, ● surface pressure and 0 surface potential are shown. Various concentrations of VSG<sub>151</sub> were injected beneath these PE monolayers (18 nmoles) as follows: 4 nmol of VSG, x surface pressure; 8 nmol of VSG, □ surface pressure; 12 nmol of VSG, Δ surface pressure and 18 nmol of VSG, ◇ surface pressure and Δ surface potential. Other conditions are as described in Fig. 5.1



### 5.1.7 Sphingomyelin

After forming the sphingomyelin (SPH) monolayer, the reproducibility of the  $\pi - A$  isotherm was tested by alternately expanding and compressing the monolayer. Reproducibility of the isotherms was the criterion used for a stable monolayer, and again care was taken not to exceed the collapse pressure. The shape of the  $\pi - A$  isotherm of sphingomyelin is similar to that for a compressible film (Figure 5.7), although Shinitzky *et al.* (1978) have shown that natural sphingomyelins are less fluid than natural phospholipids; they measured fluidity by fluorescence polarization.

The curve of surface potential versus area for sphingomyelin rises continuously until it reaches a maximum around  $350 \pm 10$  mV, close to the minimum area. It is interesting to note that a value of 250 mV was found at pH 6.8, and 300 mV at pH 8. Nevertheless, those values are below those given by Colacicco (1973), (600 mV) for cations or polyamines bound to SPH as contaminants.

Addition of VSG to SPH monolayers was carried out at  $\sim 100 \text{ \AA}^2$ , and the reactants allowed to interact for 40 to 60 minutes. Figure 5.7 shows that there is no detectable interaction between VSG and SPH at a VSG : lipid molar ratio of 2 : 9. This VSG/lipid ratio has been used for other phospholipids, e.g., Figure 5.1b where small changes in surface pressure were observed. The demonstration of no interaction which was independent of the way of adding VSG to the SPH monolayer, could be shown by adding antigen either by touching the lipid surface or by injecting beneath the film. The  $\pi - A$  isotherm of sphingomyelin was never displaced by the addition of VSG.

The  $\Delta V - A$  isotherm in most of the experiments at pH 6.8 maintained a difference about +30 to +40 mV, meanwhile at pH 8 this

Fig. 5.7a

Sphingomyelin (18 nmol) monolayer was spread at the air water interface, 0 surface pressure and 0 surface potential are shown. After injecting 4 nmol of VSG beneath this lipid film,  $\Delta$  surface pressure and  $\blacktriangle$  surface potential were determined. Subphase pH 6.8.

Fig. 5.7b

4 nmol of VSG was injected beneath a preformed sphingomyelin monolayer (18 nmol) and the procedure was as above, except that the subphase pH was 8. The subphase composition was 10 mM Tris, 145 mM KCl.

Fig. 5.7.a.

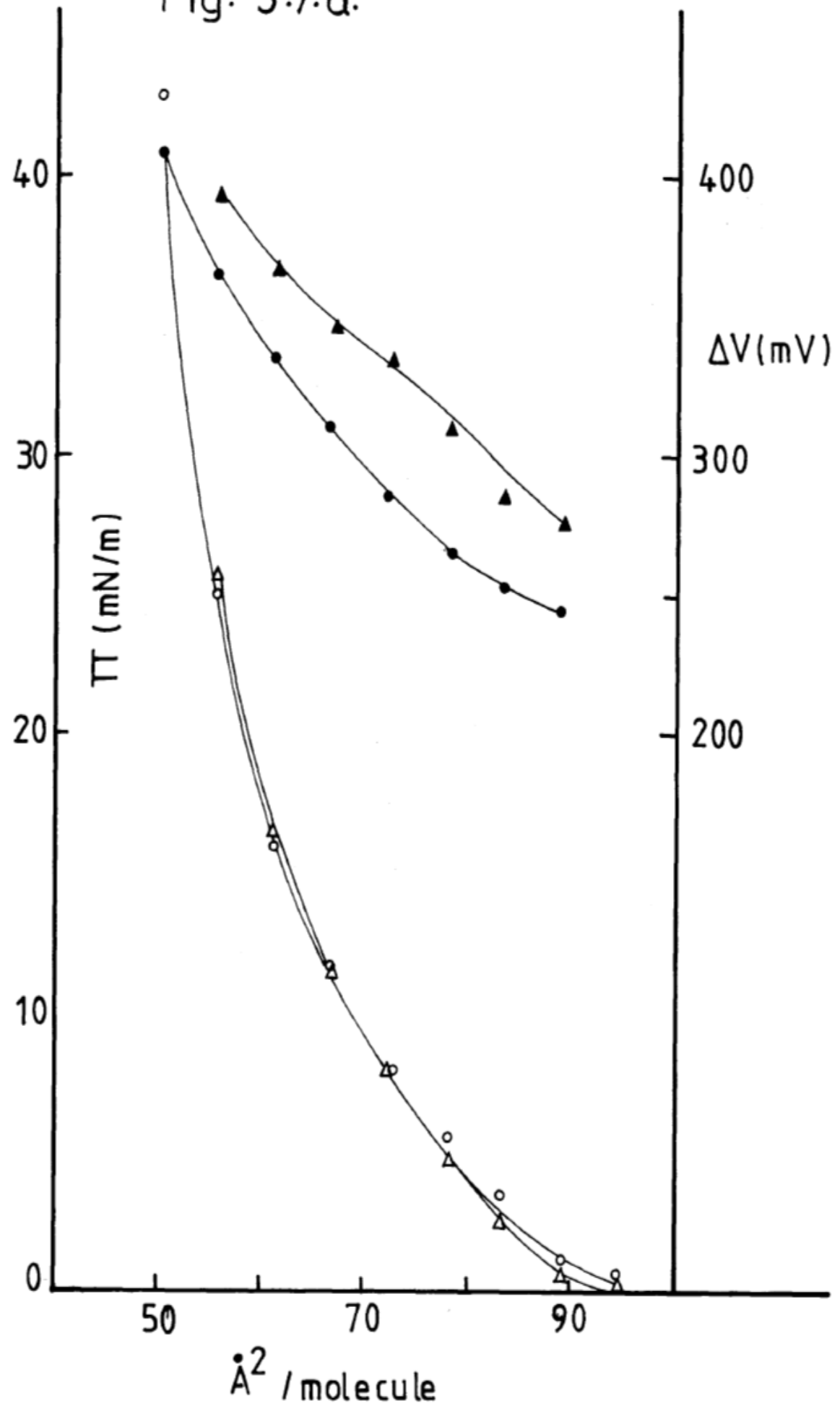
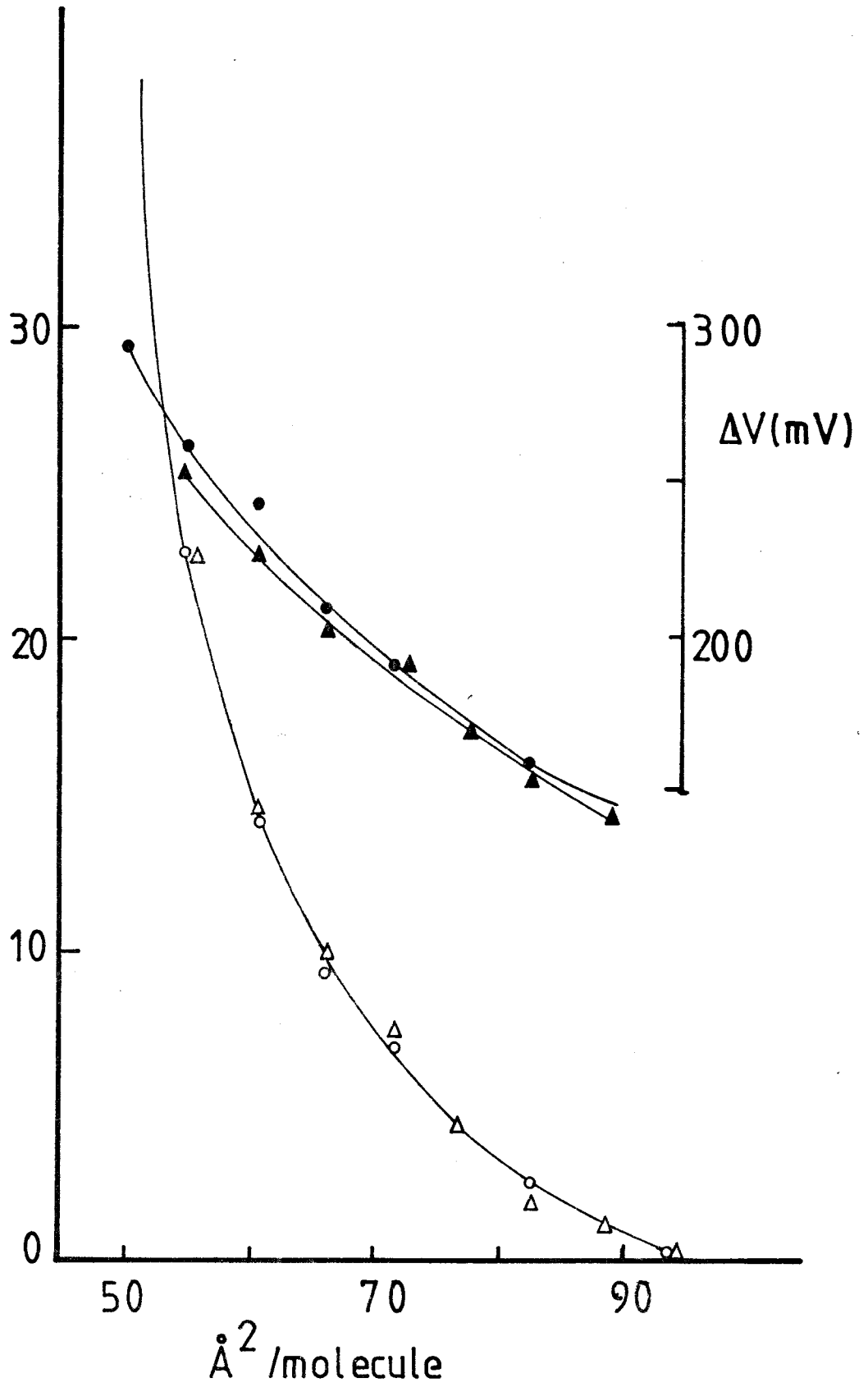




Fig. 5.7. b.



diminished by +15 mV (Figures 5.7a and 5.7b). At pH 7.4 the  $\Delta V - A$  isotherm resembles that at pH 8 (not shown).

The bulk phase was modified changing its ionic strength<sup>1</sup> from 0.157 M to 0.011 M. It is expected that if the interaction between SPH and VSG is by electrostatic means, then, at low ionic strength that interaction should be enhanced (Kimelberg et al., 1971). Experiments carried out under these conditions, however, did not produce any effect either in  $\pi - A$  or in  $\Delta V - A$  isotherms. As will be seen later, the SPH - VSG interaction was only effected if VSG was previously dissolved in presence of sodium cholate and then added to the SPH monolayer.

## 5.2 Interaction of VSG with sterol monolayers

Sterols have the basic structure shown in Figure 7.1 (see Section 7.2), additional groups such as methyl groups and double bonds confer different chemical properties.

Cholesterol and ergosterol were the sterols selected for these experiments; both sterols, cholesterol and ergosterol have been found to be present as the main sterols of trypanosome bloodstream forms and culture forms respectively (Dixon et al., 1972). Cholesterol is the major sterol of the bloodstream form of Trypanosoma brucei rhodesiense

1) Ionic strength is a measure of the intensity of the electric field in the solution. For instance the electrostatic force between a pair of doubly charged ions is four times the force between a pair carrying unit charges. The definition of ionic strength takes into account the charge of the ions as well as their respective concentrations:

$$\mu = 1/2 \sum_i m_i Z_i^2$$

$m$  is the molal concentration of each ion and  $Z_i$  is its charge. In dilute solutions of an ionic compound, the properties such as the activity coefficients, rates of ionic reactions, become functions of ion strength.

(mainly as esterified sterol), it was found in large amounts in the short stumpy form, e.g., 20% (w/w) of total lipids (Venkatesan & Gerrod, 1976). The use of other sterols is shown in section 7.1.1 where the affinity of VSG for sterol is studied.

### 5.2.1 Cholesterol monolayers

Cholesterol monolayers were formed at the air-water interface, with a subphase of pH 6.8 (composition - see section 4.9.2). The  $\pi$  - A isotherm for cholesterol (Figure 5.8) corresponded to the values in the literature (Demel & De Kruyff, 1976), this monolayer occupies only small areas per molecule ( $39 \text{ \AA}^2$ ), and is very incompressible, consistent with it being a condensed monolayer. At relatively high areas per molecule ( $> 40 \text{ \AA}^2$ ) the surface potential underwent a continuous oscillation  $\pm 50 \text{ mV}$ . This only became stable when the area per molecule was reduced to values close to the minimum area ( $39 \text{ \AA}^2$ ); the value of surface potential at this area was  $420 \pm 10 \text{ mV}$ .

The type of surface potential fluctuation described above has also been observed for phospholipids at relative large area per molecule. Phillips & Chapman (1968) have explained this fluctuation for PC and PE as the reflection of the physical state, which may be a liquid expanded phase rather than a vapour expanded phase. A more satisfactory explanation, however, comes from Adamson (1967) who suggested that cohesive inter-chain forces could predominate among the film-forming molecules at the higher surface areas, leading to the formation of clusters. This is interpreted as an irregular distribution of molecules at the water surface. In this case,  $\Delta V$  which is the resultant of several partially compensating effects, namely, dipole moments and area per molecule, will reflect such irregularity.

Fig. 5.8a

Cholesterol monolayer (25 nmoles) formed at the air-water interface, ( $\odot$ ) surface pressure, ( $\bullet$ ) surface potential. The effect of various concentrations of VSG in surface pressure and surface potential were also determined. 1.6 nmol of VSG, ( $\circ$ ) surface pressure, ( $\ominus$ ) surface potential; 4 nmol of VSG, ( $\triangle$ ) surface pressure, ( $\blacktriangle$ ) surface potential; 8 nmol of VSG, ( $\square$ ) surface pressure, ( $\blacksquare$ ) surface potential, and 12 nmol of VSG, ( $\times$ ) surface pressure and surface potential. Subphase pH 6.8.

Fig. 5.8b

Effect of lower concentrations than 1 nmol of VSG injected beneath cholesterol monolayers (25 nmoles). 0.16 nmol of VSG ( $\triangle$ ) surface pressure and surface potential; 0.32 nmol of VSG ( $\times$ ) surface pressure and surface potential and 0.8 nmol of VSG, ( $\circ$ ) surface pressure and surface potential.

Fig. 5.8.a

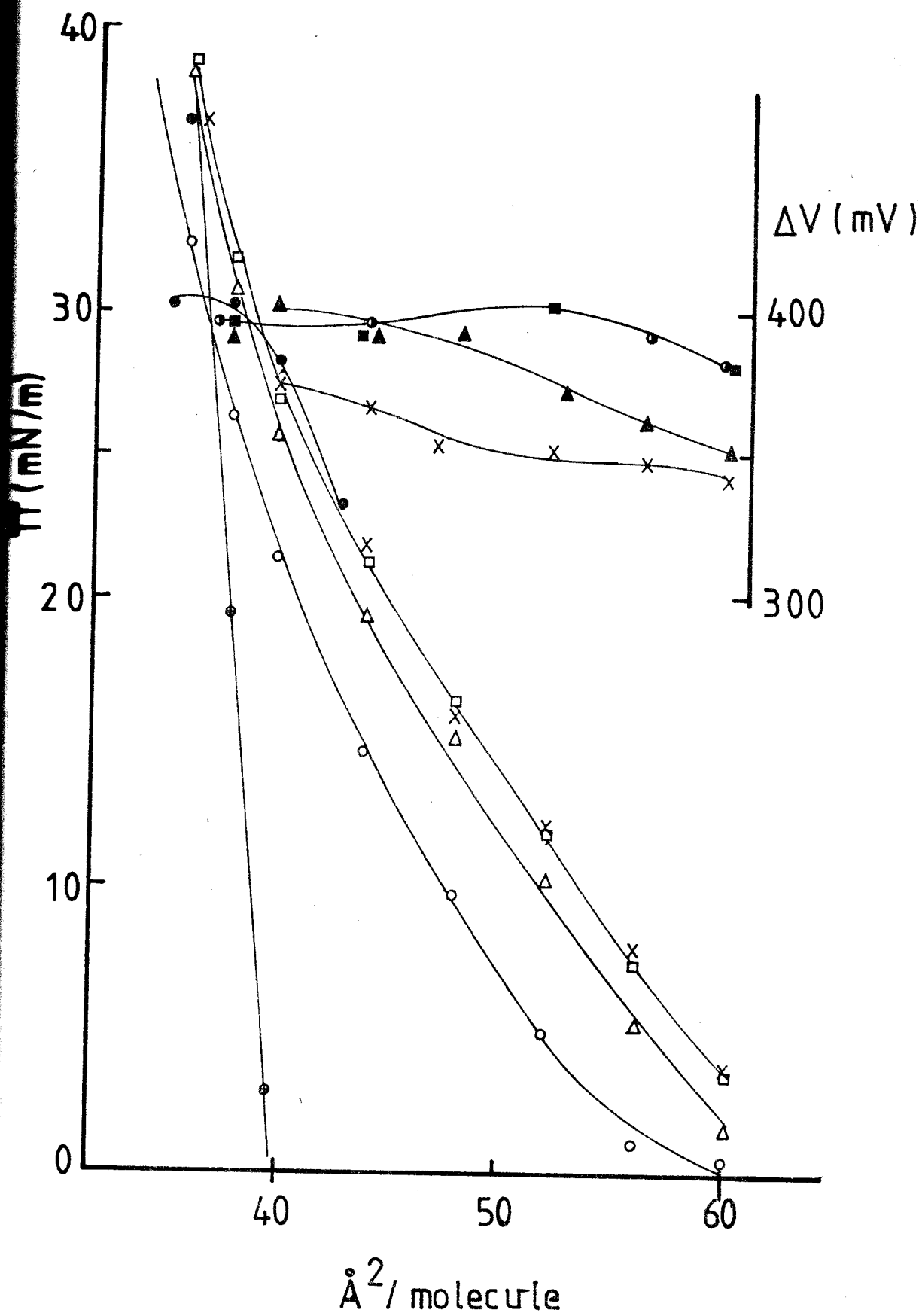
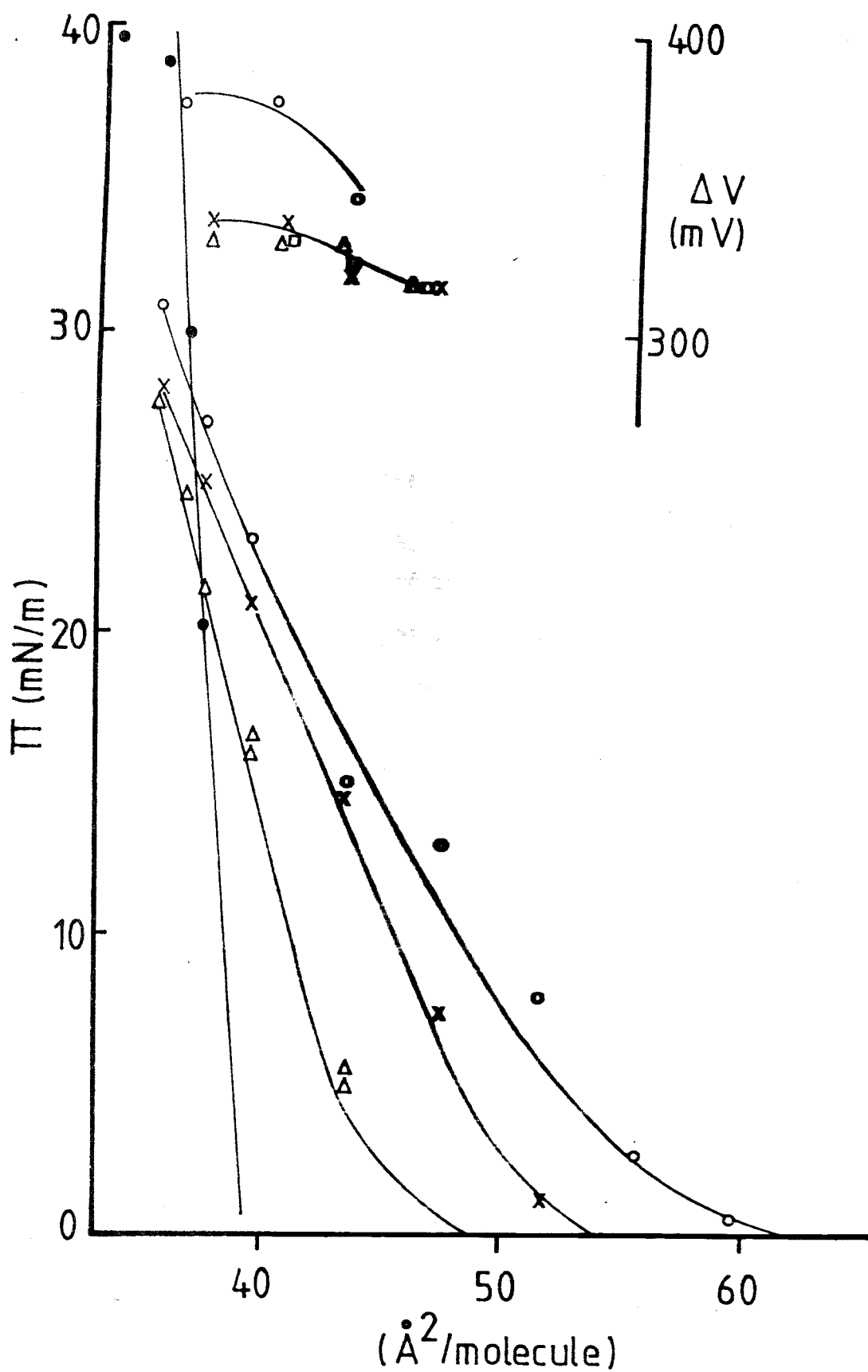


Fig. 5.8.b



Addition of VSG to the cholesterol monolayer produced a very significant change in the  $\pi - A$  isotherm, which was greatly displaced and its slope reduced considerably. This displacement could be interpreted in terms of the transition from a condensed to an expanded film. The  $\Delta V - A$  isotherm for cholesterol in the presence of VSG showed a positive increase in  $\Delta V$  in comparison with cholesterol alone at equivalent areas per molecule of cholesterol higher than  $40 \text{ \AA}^2$ . When this area was reduced to the limiting area for cholesterol,  $\Delta V$  did not increase and showed an average value equal or lower than that observed for cholesterol alone (350 mV). The displacement of the CHL  $\pi - A$  curve by VSG can be interpreted as a much stronger interaction between CHL and VSG than that observed for any of the other phospholipids. As shown later, the  $\Delta \pi_{\text{VSG}}$  for cholesterol from these curves differs in magnitude from those of the phospholipids for the same VSG concentration. Furthermore, using different concentrations of VSG led to different isotherms. But the molar ratio of VSG:CHL 1:2 appears to represent saturation of the cholesterol monolayer; remarkably, however, the low VSG concentration i.e.; 1.6 pmol/ml (VSG:CHL 1:156) which was able to displace the CHL  $\pi - A$  isotherm (Figure 5.8b) was not able to alter the phospholipid  $\pi - A$  isotherm.

### 5.2.2 Ergosterol monolayers

Ergosterol is found in nature as the main sterol in insects; it differs in chemical structure from cholesterol by the presence of a second double bond 7-8 in the cyclopentanophenanthrene nucleus. Also by a double bond 24-25 in the side chain (see diagram in section 7.2. A solution of ergosterol (1 mM in chloroform) was prepared freshly and the experimental procedures accomplished under yellow light (Kodak safelight filter, 'Wratten' series OB) to prevent oxidation. The ergosterol monolayer spread at the air-water interface corresponded

to a condensed monolayer; its force-area curve exhibited a very limited compressibility area as shown in Figure 5.9. The ERG  $\pi - A$  isotherm, although resembling that of cholesterol, shows small significant differences which can be attributed to the presence of the two double bonds in the sterol nucleus (Demel *et al.*, 1972). Thus the area per molecule is slightly increased at low surface pressure which provides a compressibility area of about  $5 \text{ \AA}^2$ , and the collapse pressure is reduced to about 32 nM/m, compared with cholesterol.

The ERG  $\Delta V - A$  isotherm (Figure 5.9), exhibited considerable fluctuations in mV at high surface area probably reflecting the gaseous-liquid transition;  $\Delta V$  only became stable at the limiting area. The average values of  $\Delta V$  observed at this area ( $36 \text{ \AA}^2$ ) were about  $550 \pm 10$  mV.

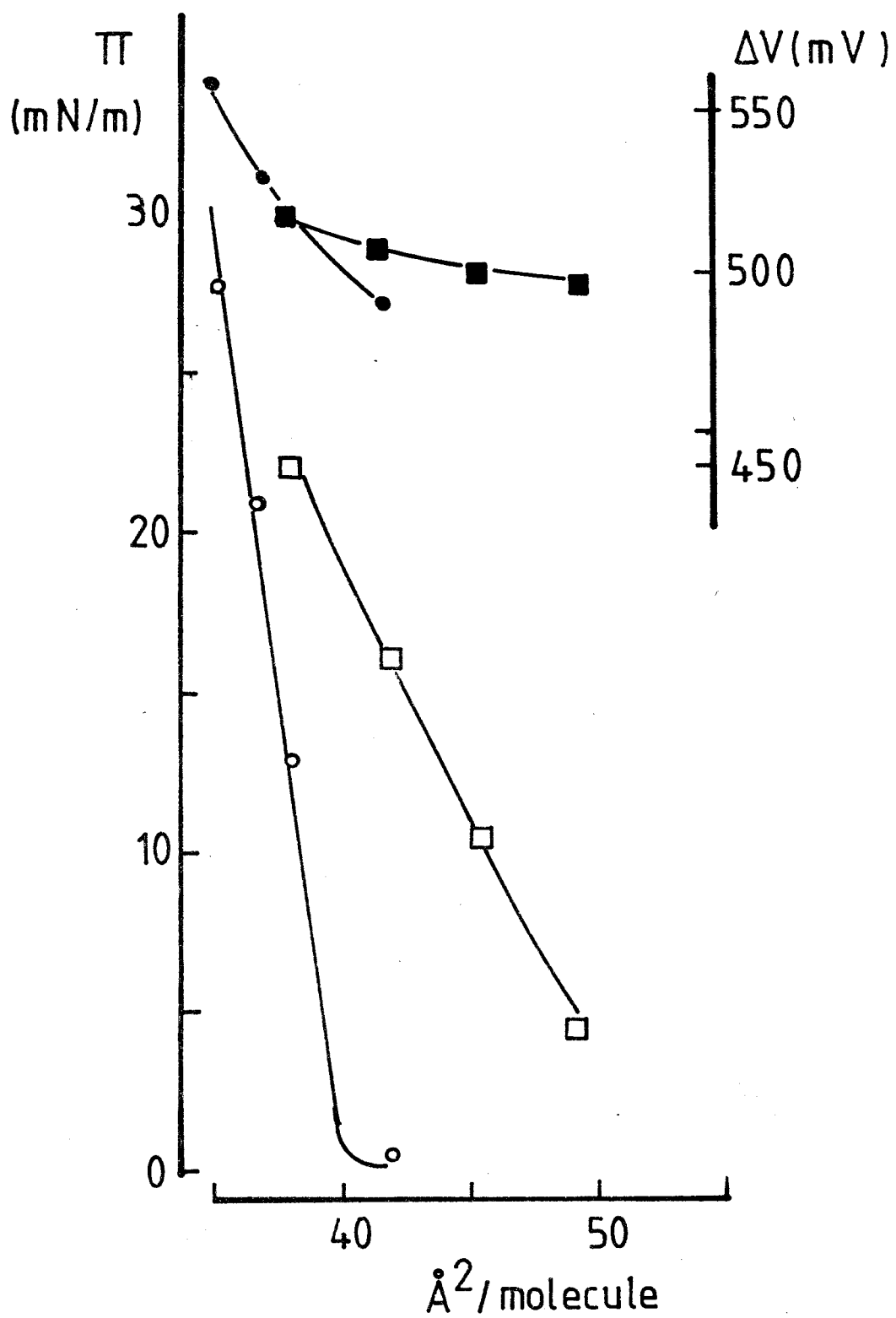
Introduction of VSG to ergosterol monolayers brought about a marked displacement of the force-area curves (as observed with CHL), which transformed the ergosterol physical state from a condensed film to an expanded film. Surface potentials were also consistent with the findings from the  $\pi - A$  isotherm of the ERG-VSG interaction. At large area per molecule the  $\Delta V$  exhibited higher and stable values than that observed for ergosterol alone, suggesting the formation of a mixed film with the properties of an expanded liquid phase. When the ERG-VSG film was compressed to the ERG minimum area,  $\Delta V$  did not increase to greater values than those observed for ERG alone (Figure 5.9). This effect was reproducible in different experiments; a few of them showed a similar  $\Delta V$  coincident with that observed for ERG alone at this area ( $36 \text{ \AA}^2$ ). This  $\Delta V$  ( $\sim 500$  mV) was never higher than that for ERG at  $36 \text{ \AA}^2$ /molecule. This suggests that VSG can be squeezed out of the monolayer, but a further, more detailed explanation would require



Fig. 5.9

Ergosterol monolayer (26 nmoles), (○) surface pressure, (●) surface potential. After injecting 1.5 nmol of VSG, (□) surface pressure, surface potential. Subphase pH 6.8.

Fig. 5.9.



knowledge of the equilibrium spreading pressure for VSG; although bearing in mind that if VSG is spread at the air-water interface the molecule would completely unfold, this can be avoided if the spreading is effected in presence of a lipid monolayer. These considerations about the contributions in surface pressure and surface potential of VSG to the 'mixed VSG-lipid film' are examined in sections 5.3, 5.4 and the discussion of this Chapter.

### 5.3 Antigen alone at the air-water interface

These experiments were aimed at investigating if VSG injected into an aqueous buffer could reach the interface, and secondly if VSG can spread on the water surface and form a stable monolayer. The property of a protein which results in its presence at the air-water interface from the bulk solution is called adsorption. A protein in the bulk solution would reach the interface by a process of diffusion. McRitchie (1978) has shown that there is a relation between the rate of adsorption and the diffusion coefficient of BSA. The importance of the property of adsorption resides in that not all proteins are able to adsorb to the interface since it depends on the proteins' ability to unfold (Colacicco et al., 1977).

The adsorption of VSG at the air-water interface was studied by adding increasing amounts of antigen to the bulk solution and allowing adsorption to take place for 60 minutes. The results of recording surface potential and surface pressure are shown in Figure 5.10a. The presence of VSG at the interface was detected early on by changes in surface potential, even at  $0.4 \text{ m}^2/\text{mg}$  ( $0.5 \text{ } \mu\text{g}/\text{ml}$ );  $\Delta V$  was 100 mV (not shown). The effect of increasing the VSG concentration is reflected by a gradual and limited  $\Delta V$  increase which reached a maximum value of

250 mV at  $0.7 \text{ m}^2/\text{mg}$ ; subsequent increase in VSG concentration did not raise this value suggesting that no more VSG was incorporated at the interface.

Two possible reasons for the fact that no increase in  $\Delta V$  followed the increase in the VSG concentration in the bulk solution are as follows: (i) the formation of a first layer of antigen at the air-water interface occurs with unfolding of antigen which is spread as an insoluble monolayer of protein (Phillips & Sparks, 1980); (ii) an equilibrium is established between the molecules adsorbed at the interface and those in the bulk phase. With both procedures of adsorption and diffusion of VSG to the interface a maximum surface pressure of 5 mN/m was observed. In a similar experiment MacRichie & Alexander (1963) showed that after the formation of a BSA monolayer at the interface, the rate of adsorption of BSA molecules from the bulk solution decreased to values below those calculated from the coefficient of diffusion, indicating the presence of an energy barrier to adsorption.

The second question is whether VSG at the buffer surface could spread and form monolayers of VSG. From Figure 5.10a, it can be seen that (a) the  $\Delta V - A$  isotherm behaviour is similar to that obtained for adsorption experiments, and the plateau was also reached at near to  $0.07 \text{ m}^2/\text{mg}$ ; (b) the  $\pi - A$  isotherm shows that changes in surface pressure were slightly higher than those observed in adsorption experiments for the same range of VSG concentration (below  $10 \text{ }\mu\text{g/ml}$ ). When VSG was spread at the air-water interface and compressed, it showed no differences in the  $\pi - A$  and  $\Delta V - A$  isotherms (Figure 5.10b), compared with when VSG at a final concentration of  $10 \text{ }\mu\text{g/ml}$  was added by the first and second procedure described above. Also it is noteworthy that the shape of the  $\pi - A$  curve does not correspond to that described

for an insoluble monolayer (Adams, 1967, p. 95). Nevertheless, spreading small amounts of VSG at the water surface at zero surface pressure and after equilibration for 1 hour, the  $\pi - A$  curve obtained under those conditions resembled that of an insoluble monolayer. The  $\Delta V - A$  curve reached a value of 300 mV at 15 mN/m, which corresponds to experiments using higher amounts of VSG (see above). The  $\pi - A$  isotherm, however, varied significantly between different monolayers even for the same VSG concentration (Figure 5.10c). A possible explanation for these results is that touching the buffer surface with a very low quantity of VSG no energy barrier is formed; i.e., surface tension remains unchanged. Under those conditions the protein molecule probably spreads and unfolds more extensively (Benjamins *et al.*, 1975; Phillips & Spark, 1980).

These studies show some of the properties of VSG at the air-water interface. There was not, however, an exhaustive study of VSG forming protein monolayers; for example the method of Tunit (1960) was not used. In this respect these results cannot account for a detailed mechanism with structural changes of VSG at the interface. Nevertheless, from those results when VSG was added to the bulk solution or by spreading on touching the water surface, the following can be deduced; (i) VSG can adsorb at the air-water interface; (ii) it does not form proper monolayers at least with the methodology used here; and (iii) the shape of the  $\pi - A$  isotherm suggests that VSG is expelled into the subphase at surface pressure higher than 5 mN/m, which is also suggested by the  $\Delta V - A$  isotherms.

Fig. 5.10a

VSG<sub>121</sub> was **spread** at the air water interface either by touching the aqueous **surface**: (O) surface pressure and (●) surface potential, **or by** injecting various concentrations of VSG into the subphase: ▲ surface potential and Δ surface pressure.

Fig. 5.10b

**Force area** curves of VSG (16 nmoles) spread at the air-water interface either by touching the liquid surface or by injecting VSG into the subphase, (O) surface pressure and (●) surface potential.

Fig. 5.10c

**Force area** curves of VSG (4 nmoles) spread at the air-water interface by touching the liquid surface, (O) surface pressure and (●) surface potential.

Subphase: 10 mM Tris-Maleic acid, 145 mM KCl, pH 6.8.

Fig. 5.10.a

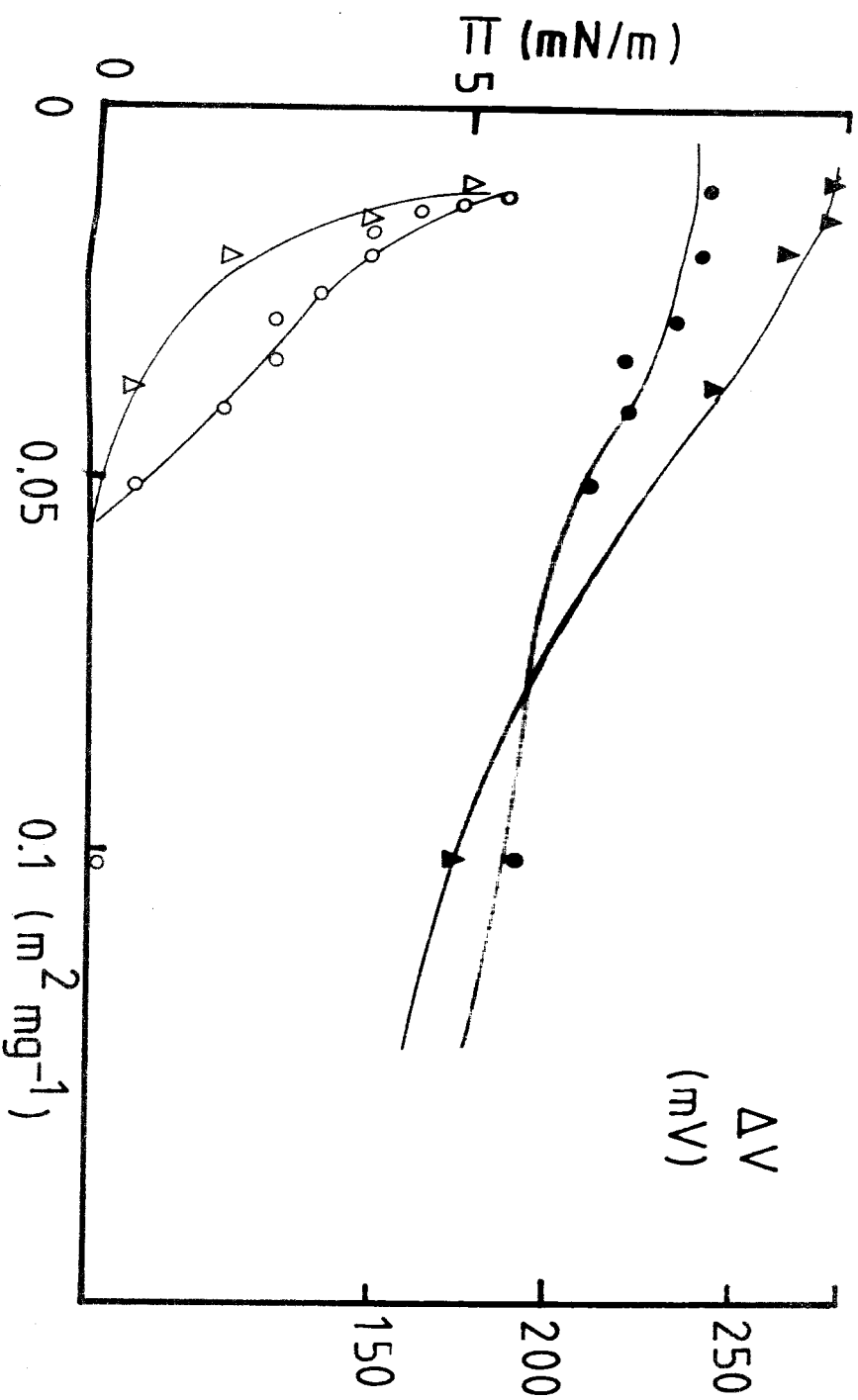


Fig. 5.10.b.

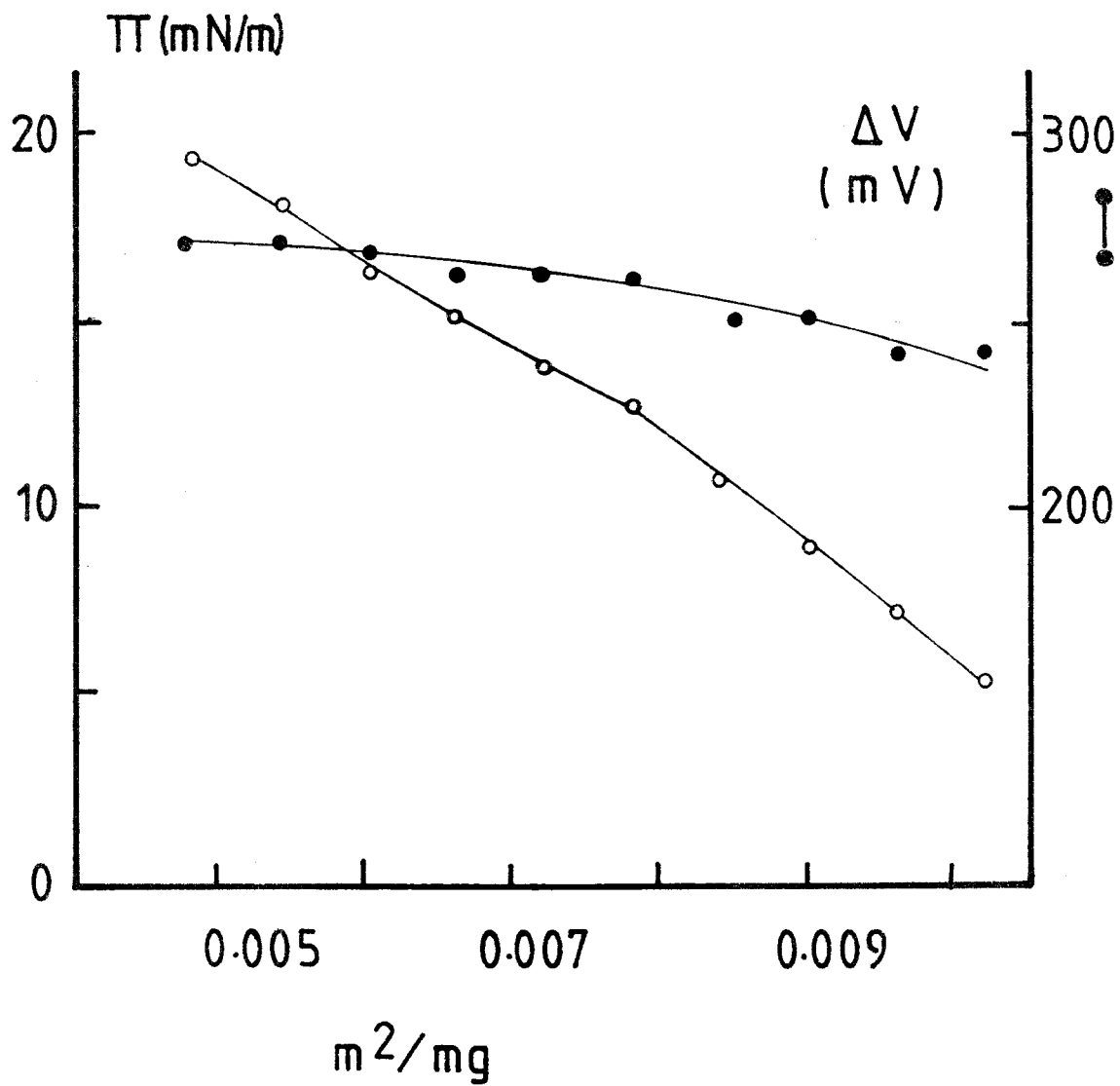
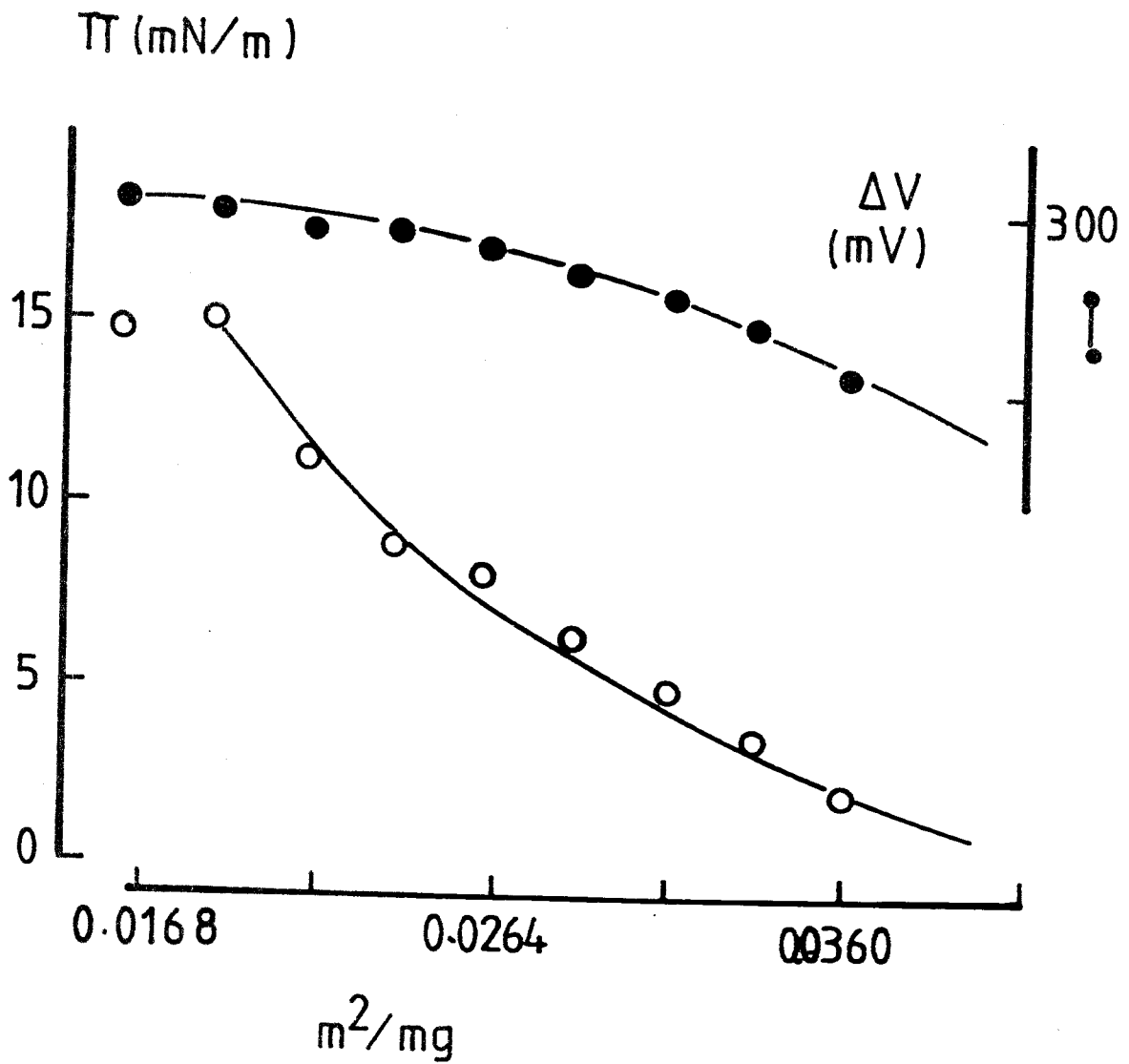




Fig. 5.10.c



#### 5.4 Quantitative approach to the antigen-lipid interaction

The properties of the different lipid monolayers and the effect of VSG on these properties has already been discussed qualitatively. The quantitative study of lipid protein interaction has proved to be of great value in this field (Bougis et al., 1981). Difficulties in doing such studies involve several biochemical, biophysical and thermodynamic principles. In monolayer systems the surface/volume ratio is small  $\approx 1 \text{ cm}^2/1 \text{ cm}^3$  as compared to liposomes,  $5 \times 10^3 - 10^4 \text{ cm}^2/\text{cm}^3$  (Verger & Pattus, 1982). Thus only a small fraction of water-soluble proteins with low hydrophobicity will bind to the lipid monolayer; high hydrophobicity will increase that binding. But to say how much, requires a direct measurement of the amount of binding to the monolayer, which is not straightforward, or an indirect assessment of binding. Even using radiolabelled proteins, consideration of denaturation of proteins adsorbed at the air-water interface not exchanging freely with molecules in the aqueous phase has to be taken into account (Phillips & Spark, 1980). Water-soluble protein molecules tend to form aggregates and this association depends on the molecule hydrophobicity (Phillips et al., 1975a; Schubert et al., 1977). Non-specific adsorption to the wall of the solid container also occurs (Verger, 1980). All of these difficulties have to be considered in any further consideration of the ratio of protein to lipid.

It seems important to clarify the use of the term 'protein hydrophobicity'. This is not a thermodynamic definition, such as that applied to amino acids; i.e., the difference between the standard unitary free energy ( $\mu_{\text{org}}^0 - \mu_{\text{w}}^0$ ) for tryptophan is -3400 cal/mole at 25°C, that figure representing the additional free energy of transfer for tryptophan from water to an organic solvent (Tanford, Chapter 7,

1973). The term 'protein hydrophobicity' is used on the basis of amino acid composition and **surface** active properties. The relatively high surface activity of a **protein** at the air-water interface is expected from the ratios of **hydrophobic** to polar amino acids (Williams, <sup>et al.,</sup> 1979; Capaldi/1972). The **surface** activity can be measured either by spreading the protein alone at the air-water interface (Boyd et al., 1973; Phillips et al., 1975; Phillips & Sparks, 1980), or by studying its interaction with **lipid films** and its effects on the lipid transition temperature (Papahadjopoulos et al., 1975; Colacicco, 1969; Cardin et al., 1982). The use of the ratio of hydrophobic to polar amino acids is not a sufficient criterion for evaluating protein hydrophobicity (Morrisett et al., 1977), and it is considered in the Discussion of this Chapter.

#### 5.4.1 The Gibbs adsorption equation

The use of thermodynamic equations, particularly the Gibbs adsorption equation in assessing the molecules adsorbed at the air-water interface has received marked criticism from some authors because of the disagreement between values observed practically and those predicted theoretically (Colacicco, 1970; Benjamin <sup>et al.,</sup> 1975; Evans et al., 1976; Phillips & Spark, 1980). This has led to proposed modifications on experimental (Pethica, 1955) and theoretical grounds (Alexander & Barnes, 1980; Motomura, 1982). It is interesting to recall the analysis of the thermodynamics of surfaces given by Willard Gibbs (1928) (see Gaines, 1966, Chapter 2; Aveyard & Haydon, 1973, Chapter 1 and Moore, 1978, Chapter 11). Considering a liquid in equilibrium with its vapour, there is a region within which the density of energy, matter and entropy undergoes a transition; this is known as the inter-

facial region. The general **tendency** to minimize the free energy is manifested for surfaces as a **reduction** in the area or a decrease in surface tension, or both. In **this** system, the surface tension is the force due to imbalanced **molecular attraction** which tends to pull molecules into the interior **of the** liquid phase, and hence to minimize the surface area.

In the Gibbs treatment **the interface** is regarded as a mathematical dividing plane (the Gibbs surface). This is illustrated in Figure 5.11. AA' is the boundary **plane for** the phase  $\alpha$ . The extensive properties of bulk  $\alpha$  are **unchanged up to** the dividing surface, and for the bulk  $\beta$  up to the surface **BB'**. SS' is an imaginary dividing surface (the Gibbs surface) **within the interfacial region** parallel to the surfaces AA' and BB' in **some arbitrary position**, designated by a superscript s. It is a **two dimensional phase** (has zero thickness and volume) with an area A. The **concentration of any component i** up to AA' is uniformly  $C_i^\alpha$  and any **component i up to BB'**, uniformly  $C_i^\beta$ . From the conservation of the **mass**

$$n_J = n_J^\alpha + n_J^\beta + n_J^S \quad \dots\dots\dots (5.2)$$

$n_J$  = number of molecules of **compound J**, the superscript indicating the phase.

The extension of the **treatment** in (5.2) can be applied to other extensive variables of the system i.e.

$$u^S = u - [u^\alpha + u^\beta] \quad \text{(surface energy)}$$

$$s^S = s - [s^\alpha + s^\beta] \quad \text{(surface entropy)}$$

Gibbs defined the adsorption of component J at the interface as

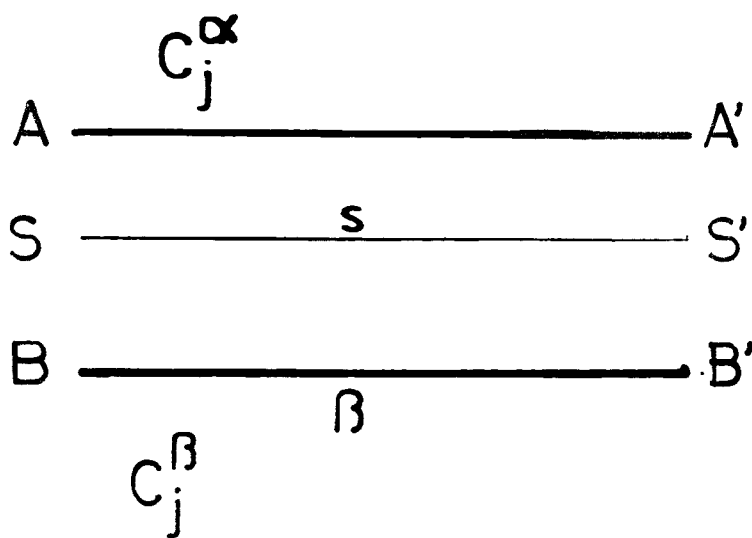


Fig. 5.11

The Gibbs dividing surface.

$$\Gamma_i = n_j^S/A \quad \dots\dots\dots (5.3)$$

This quantity has the dimensions of a surface concentration and it may be positive or negative in accord with  $n_j^S$ .

The surface Gibbs function can be written

$$dG^S = S^S dT + \gamma dA + \sum \mu_j^S dn_j^S \quad \dots\dots\dots (5.4)$$

At equilibrium,  $\mu_j^\alpha = \mu_j^\beta = \mu_j^S$  (condition of equality for chemical potential)

and at constant T (5.4) becomes

$$dG^S = \gamma dA + \sum \mu_j^S dn_j^S \quad \dots\dots\dots (5.5)$$

Integrating (4) at constant  $\gamma$  and  $\mu_j$  gives

$$G^S = \gamma A + \sum \mu_j^S n_j^S \quad \dots\dots\dots (5.6)$$

and differentiating (5.6) and comparing with (5.5) gives

$$A d\gamma + \sum n_j^S d\mu_j^S = 0 \quad \dots\dots\dots (5.7)$$

Dividing by the area (A) of the interface and introducing  $\Gamma_j$  (5.3)

$$d\gamma = -\sum \Gamma_j d\mu_j \quad \dots\dots\dots (5.8)$$

The latter is the Gibbs surface tension equation. Equation (5.8), however, cannot be used to determine the adsorption of each component from the variation in  $\gamma$ ; this was resolved by Gibbs introducing the idea of relative adsorption.

For a system of two components

$$d\gamma = -\Gamma_a d\mu_a - \Gamma_b d\mu_b \quad \dots\dots\dots (5.9)$$

If  $\Gamma_a = 0$  for that surface and  $\Gamma_b \neq 0$  equation (5.9) becomes

$$d\gamma = -\Gamma_{b,a} d\mu_b$$

$$\Gamma_{b,a} = - \frac{\delta \gamma}{\delta \mu_b} \quad \tau \quad \dots \dots \dots (5.10)$$

(5.10) is the Gibbs (relative adsorption isotherm. For a solution, or in dilute solutions,

$$d \mu_b = RT \ln cb \quad \dots \dots \dots (5.11)$$

where  $cb$  is the bulk concentration of the compound  $b$ , and (5.10) becomes

$$\Gamma_{b,a} = - \frac{1}{RT} \frac{\delta \gamma}{\delta \ln cb} \quad \tau = - \frac{cb}{RT} \frac{\delta \gamma}{\delta cb} \quad \tau \quad (5.12)$$

The application of the Gibbs adsorption isotherm (5.12) for solutions containing synthetic polymers or biopolymers has given values which differ significantly from the measured experimental surface excess ( $\Gamma$ ) (Colacicco, 1970; Phillips & Spark, 1980). These authors, however, have assumed that the adsorption of salt and water could be neglected, which is one of the requirements of equation (5.12), and they also used protein concentration rather than activity, assuming non-association of the protein molecules in the bulk phase. This discrepancy is discussed by Phillips & Sparks (1980) and Graham & Phillips (1979) for several proteins; and these authors have suggested that the primary layer of protein is adsorbed irreversibly. Thus the protein molecules appears not to exchange freely between the air-water interface and the subphase. These observations lead to the need for a re-examination of such theoretical and practical assumptions in the application of the Gibbs (relative) adsorption equation. Indeed the adsorption of protein to an insoluble monolayer in the presence of excess of neutral electrolyte, present enormous difficulties because it is not possible to control or measure the activity of the monolayer component (Eley & Hedge, 1957). Pethica (1955) attempted a solution to

this problem by modifying equation (5.12), and introducing a factor to correct for the presence of excess electrolyte,

$$\phi = \frac{a}{a} - \bar{a} \quad \dots\dots\dots (5.13)$$

$a$  is the spread area per molecule for the insoluble monolayer before adding the protein solution;  $\bar{a}$  is the partial molar area for the insoluble monolayer at the completion of the first layer of adsorbed protein, calculated as the area occupied by a lipid molecule in a pure lipid monolayer at the same surface pressure.

The final equation is

$$d \pi = \phi RT \Gamma d \log c \quad \dots\dots\dots (5.14)$$

It is noteworthy that Pethica's equation was used in the studies of cholesterol film penetration by sodium dodecyl sulphate; and that the theoretical value was close to the experimental one. Eley & Hedge (1957) also applied the Gibbs equation (5.14), as modified by Pethica, to studies of the adsorption of proteins to cholesterol and stearic acid monolayers, with a subphase of ionic strength 0.15 M. Alexander & Barnes (1980), however, have criticised the validity of Pethica's modification to the Gibbs (relative) adsorption isotherm. The arguments were theoretical ones and the authors have derived a new equation whose applicability has been restricted to the penetration of cholesterol monolayers by sodium dodecyl sulphate. Any possible application to a system containing lipid and protein would require some other considerations such as reversibility of the protein adsorption and its relative surface area occupied in the lipid monolayer which are not discussed here. Another strong criticism was made by Motomura et al. (1982) who objected that Pethica's equation is incorrect



thermodynamically; however, the emphasis on such treatment of equation (5.14) has been theoretical and lacks experimental support, making further consideration difficult.

From the above discussion it can be seen that a definitive equation for relative interfacial adsorption has yet to be achieved. Pethica's equation (5.14) appears to be the closest approximation available and reasonably consistent with the experimental results. Therefore the modified Gibbs adsorption isotherm (equation 5.14), although the problems associated with it have not been completely resolved, looks the most feasible relationship for calculating the VSG adsorbed at an interface consisting of an insoluble monolayer of lipid and excess neutral electrolyte.

#### Penetration of lipid monolayers at low surface pressure by VSG 151

Monolayers of EYPC (18 nmol), PE (18 nmol) and CHL (25 nmol) were spread at the air-water interface and their stability checked by determining the force versus area curves and the surface potential versus area curves. The monolayers were compressed to  $2 \text{ m.Nm}^{-1}$  and allowed to equilibrate for 10 minutes; small variations of  $\pm 0.6 \text{ m.Nm}^{-1}$  were observed. In particular, cholesterol was always the most difficult film to set up; on the one hand it had the advantage that contaminant surfactives produced a considerable increase of surface pressure; on the other hand, because of its restricted compressibility arising from its condensed state, the setting up of a monolayer at low surface pressure took a long time. Adsorption of VSG at the air-water interface in the presence of an insoluble lipid monolayer, was carried out as follows. VSG was injected under the lipid film with a subphase containing buffer pH 6.8, corresponding to the VSG isoelectric

point. Concentrations of VSG higher than 0.08 nmol/ml required about 2 hours to reach an equilibrium surface pressure (constant  $\Delta\pi$  values). It is noteworthy that addition of VSG by touching the 'air-(water)-lipid interface' yielded similar  $\Delta\pi$  values to those when VSG was injected beneath the film (up to 1  $\mu\text{g/ml}$  or approximately 0.016 nmol/ml). Any fixed amount of VSG could be added as aliquots at intervals up to 1 hour (monolayer exposed for not longer than 3 hours), and the  $\Delta\pi$  value after the last addition corresponded to that observed when the total amount of VSG was added in one step. Figure 5.12 summarises the results of film penetration by various concentrations of VSG. The net change in surface pressure is calculated using equation (5.1)

$$[ \Delta\pi_{\text{net}} = \pi_{\text{Lipid-VSG}} - \pi_{\text{Lipid}} (2 \text{ mNm}^{-1}) ],$$

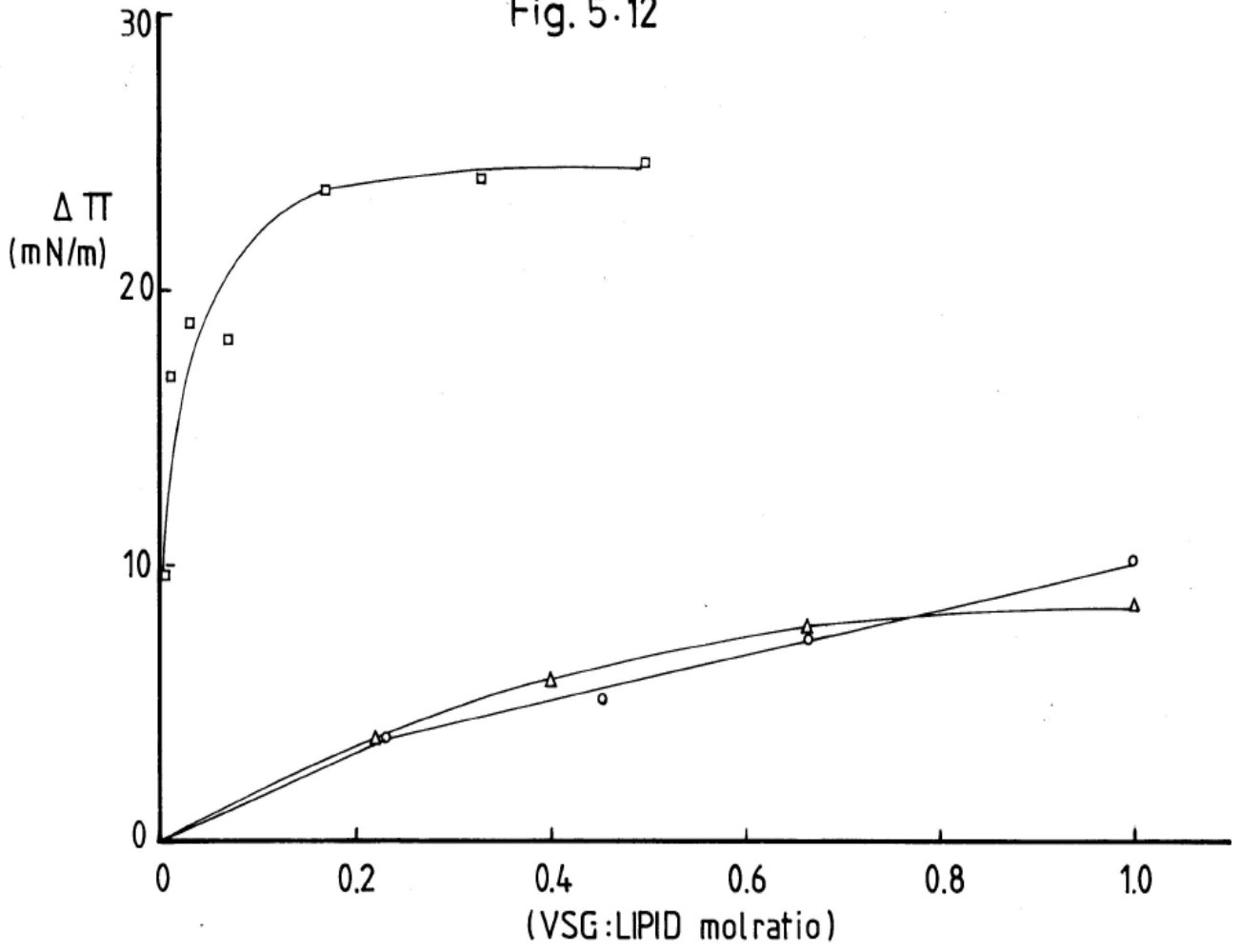
$\pi_{\text{Lipid-VSG}}$  being the change in surface pressure after adding VSG at the initial surface pressure with lipid alone ( $\pi_{\text{Lipid}}$ ). The interaction with cholesterol is about 4 times greater than that with PC or PE at a 1:2 VSG:Lipid ratio; in addition the CHL curve reaches a plateau at lower ratios of VSG:lipid.

The point at which this curve becomes discontinuous was taken as corresponding to the quantity of VSG required to form the first layer (Eley & Hedge, 1956) and the values obtained are shown in Table 1(a). The plot of the net change in surface pressure versus  $\log c$  ( $c$  is the VSG concentration in nmol/ml) also permits calculation of  $d\pi/d \log c$ , the slope being that at the point of inflexion where a second layer of protein is assumed to become adsorbed (not shown). The calculated values for  $d\pi/d \log c$  are shown in Table 1(b); this slope was used to calculate the surface excess ( $\Gamma$ ) of VSG in various lipid monolayers

**Fig. 5.12**

**Film penetration** experiments. At an initial surface pressure of **2 mN/m** various concentrations of VSG were injected beneath the following films: ( $\square$ ) cholesterol, ( $\Delta$ ) phosphatidyl ethanolamine and (O) egg yolk phosphatidyl choline. Changes in surface pressure ( $\Delta\pi$ ) was determined after 1 hr of incubation or until reaching stable values.

Fig. 5.12



as shown in Table 1(b) at 20°C. The number of penetrating units of VSG was calculated from the modified Gibbs equation as follows; the average molecular weight of 63,000 VSG (from Auffret & Turner, 1981) contains approximately 548 amino acid units, and the mean area per amino acid is  $15 \text{ \AA}^2$  (references given in section 5.4.2); then the number of penetrating amino acids per molecule of VSG is given by,

$$(548 \times 15) \times (\tau) = \text{No units.}$$

#### 5.4.2 Geometric Model

A further method for calculating the number of penetrating units is by considering a geometric model. This model, which has been used by Ely & Hedge (1957), is applied here with certain modifications. In the original model it was considered that all the protein molecules were adsorbed to the lipid surface. In this case, only the first layer of VSG will be considered adsorbed at the interface. Available surface area is defined as the total area of the trough minus the area occupied by the complete packing of lipid molecules. Then assuming the average area for an amino acid to be  $15 \text{ \AA}^2$  (Yamashita & Bull, 1967; Phillips, 1975a; Shen *et al.*, 1977) a value observed for completely unfolded proteins spread at the air-water interface, the antigen adsorbed at the available surface area ( $\text{\AA}^2/\text{molecule}$ ) was divided by  $15 \text{ \AA}^2$  and the resulting value represents the number of units penetrating the lipid monolayer. The values for PE, EYPC and CHL are given in Table 1(b).

#### 5.4.3 The Lateral Compressibility Coefficient ( $\delta$ )

The equation describing the Lateral Compressibility Coefficient, defined by Bull (1964) is given by

Table 1(a) Lipid-VSG interaction

Lipid	VSG First Layer (nmol)	VSG/Lipid Molar Ratio	$\Delta\pi_{\text{net}}$ mN/m	Partial Available Area ( $\text{\AA}^2$ )
CHL	2.2	1:11.4	18	$3 \times 10^{16}$
PE	8.0	1:4.5	4	$5.4 \times 10^{16}$
EYPC	8.0	1:4.5	4	$5.7 \times 10^{16}$

Table 1(b)

Lipid	Slope $d\pi/d \log c$	$\phi$ $a/a-\bar{a}$	$\Gamma$ molecule/ $\text{A}^2$	Gibbs Equation	Number of penetrating units of VSG			
					Geometric Model	$\delta$	RIA	Miscibility
CHL	22.3	20	$1.9 \times 10^{-3}$	16	2	9	6	11
PE	6.64	18.4	$6.2 \times 10^{-4}$	5	1	9	2	9
EYPC	4.65	21	$3.8 \times 10^{-4}$	3	1	9	3	6

The values of various parameters are summarised in this table. The calculations and their corresponding sections are described below.

Partial available area is defined as the spread lipid area (A) when  $\pi = 2 \text{ mN/m}$  minus the partial molecule area ( $\bar{a}$ ).  $\Gamma$  was calculated from equation (5.14). Geometric model is defined in Section 5.4.2. Relative Increase Area (RIA) is defined in Section 5.4.4. Miscibility is defined in Section 5.4.5. Coefficient of Lateral Compressibility ( $\delta$ ) is defined in Section 5.4.3.

$$\delta = - \frac{1}{A} \times \frac{dA}{d\pi} \dots\dots\dots (5.15)$$

This coefficient,  $\delta$ , can be calculated from the force vs area curve of a monolayer film at the air-water interface by the use of the above equation; A is the area of the film in  $\text{m}^2 \text{mg}^{-1}$  (for a protein monolayer) and  $\pi$  is in  $\text{mNm}^{-1}$ .

When the coefficient of lateral compressibility is plotted against the area of the film a well-defined minimum is usually observed. This minimum of compressibility corresponds to the smallest area (limiting area) to which a film can be compressed without partial collapse of the film occurring. For different protein monolayers the reported value is  $0.8 \text{ m}^2 \text{ mg}^{-1}$  (Colacicco, 1969; Phillips et al., 1975a). Application of the compressibility coefficient to a mixed system such as lipid-protein allows the assessment of the interaction between the components at both low and high surface pressure and, in addition, the effect of introducing known variables; for example, lipids in different physical states, changes in protein concentration, denaturation etc.

et al.  
Phillips (1975b) has observed a relationship between penetration of  $\beta$ -casein into phospholipid monolayers and bilayer membranes that is dependent on the liquid-crystalline state. Enhancing the lateral compressibility at boundary layers facilitates the insertion of the hydrophobic protein (Phillips, 1975b; Op Den Kamp, 1974). Another property of a lipid-protein system is that when adsorption of a hydrophobic protein occurs partial or total denaturation can be avoided, depending on the initial surface pressure (Verger & Pattus, 1982). Under these conditions, the protein conformation which interacts with lipids may correspond to its biological native form.



Lipid monolayers were set up at an initial surface pressure of  $2 \text{ mNm}^{-1}$  and VSG was added by touching the lipid surface; the initial surface pressure was kept constant by moving the barrier of the trough. The time allowed for interaction was 1 hour, and then a force-area curve was determined. Care was taken with the compression of the monolayer, and the time allowed for equilibrium to be attained was at least 5 minutes per surface area measurement.

The data for equation (5.15) were calculated as follows:  $A_0$  is the available area after subtracting that occupied by the lipid molecules and dividing by the adsorbed VSG (Figure 5.13). In this calculation complete adsorption of VSG was assumed to have taken place at the lipid-water interface. For this purpose approximate concentrations of VSG capable of forming the first antigen layer beneath the lipid film were used (shown in Table 1(a)).

A complete set of data was produced from the force-area curve of lipid-VSG monolayer and is expressed in the form of a plot of the coefficient of lateral compressibility ( $\delta$ ,  $\text{mN}$ ) versus surface area per VSG ( $A$ ,  $\text{\AA}^2/\text{molecule}$ ). The  $\delta$  values for the mixed films of VSG with PE and EYPC are shown in Figure 5.14.

The minimal surface areas fluctuate between 8 and  $15 \times 10^{-3} \text{ m}^2 \text{ mg}^{-1}$ ; in any case these values are far below those reported for protein films at the air-water interface ( $0.8 \text{ m}^2 \text{ mg}^{-1}$ ) (Malcolm, 1973). The minimum  $\delta$  value for phospholipids was best determined with 0.25 mg VSG; if lower concentrations of VSG were used the displacement of the force-area curve became too small to be measured accurately. On the other hand amounts of VSG above 0.25 mg showed less well-defined minima for the  $\delta$  values. The values of total sur-

Fig. 5.13

The **surface** pressure of the lipid-VSG monolayer was determined and is plotted against the area per mg of VSG. The latter was calculated as the available surface area (the area left after subtracting that occupied by the lipid molecules), divided by the absorbed VSG. The bar indicates the range of curves which can be obtained using different concentrations of VSG. For cholesterol the range was between 0.1 and 0.25 mg of VSG, and from 0.2 to 0.50 mg of VSG for phosphatidyl ethanolamine and phosphatidyl choline.

Fig.5.13

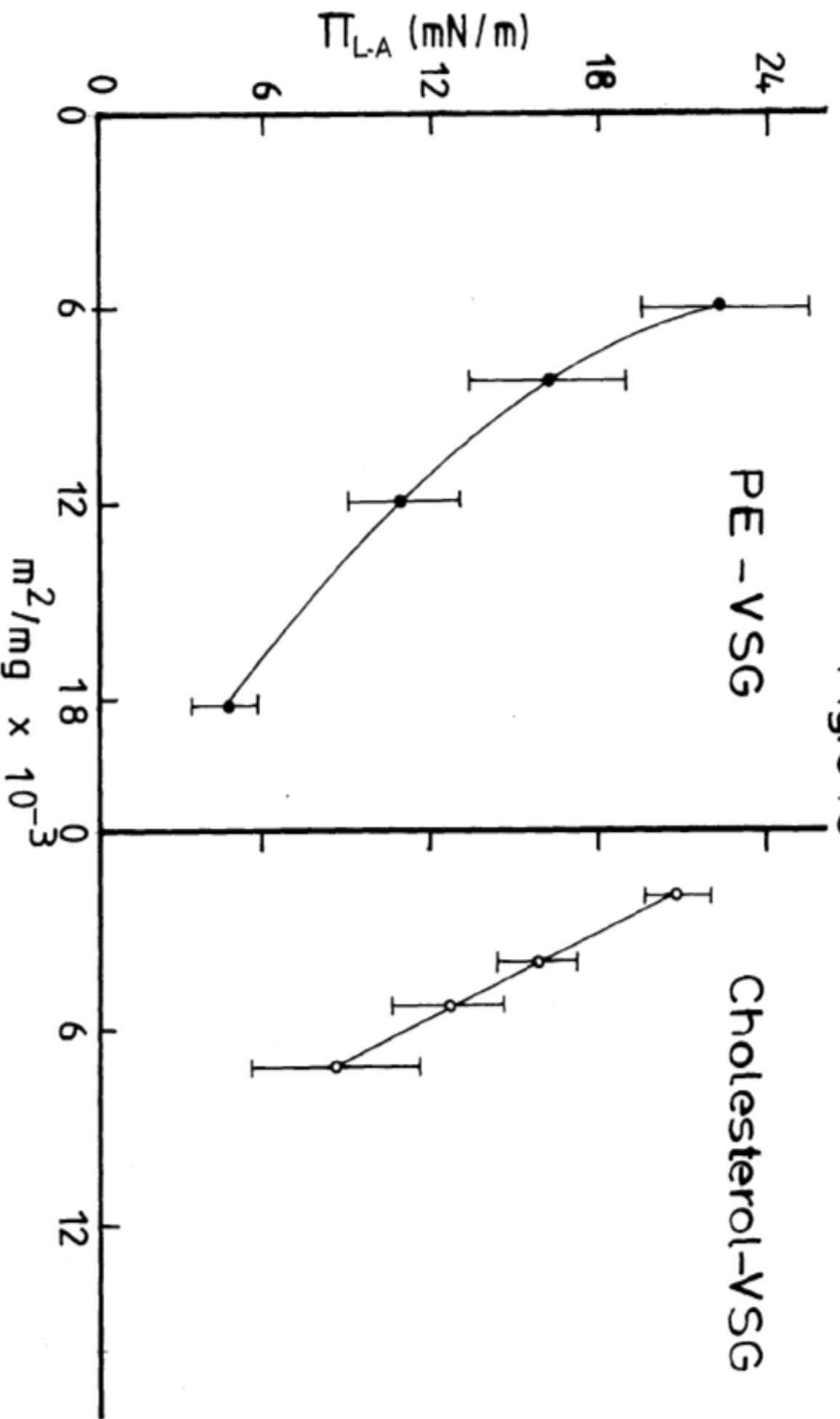


Fig. 5.14 (a) and (b)

The coefficient of lateral compressibility ( $\delta$ ) was calculated from the slopes of the force-area curves for phosphatidyl choline-VSG, phosphatidyl ethanolamine-VSG and cholesterol-VSG monolayers, using equation (5.15). The total surface pressure for VSG at the surface area per VSG corresponding to that of the minimum lateral compressibility was estimated using Fig. 5.13.

Fig. 5.14.a

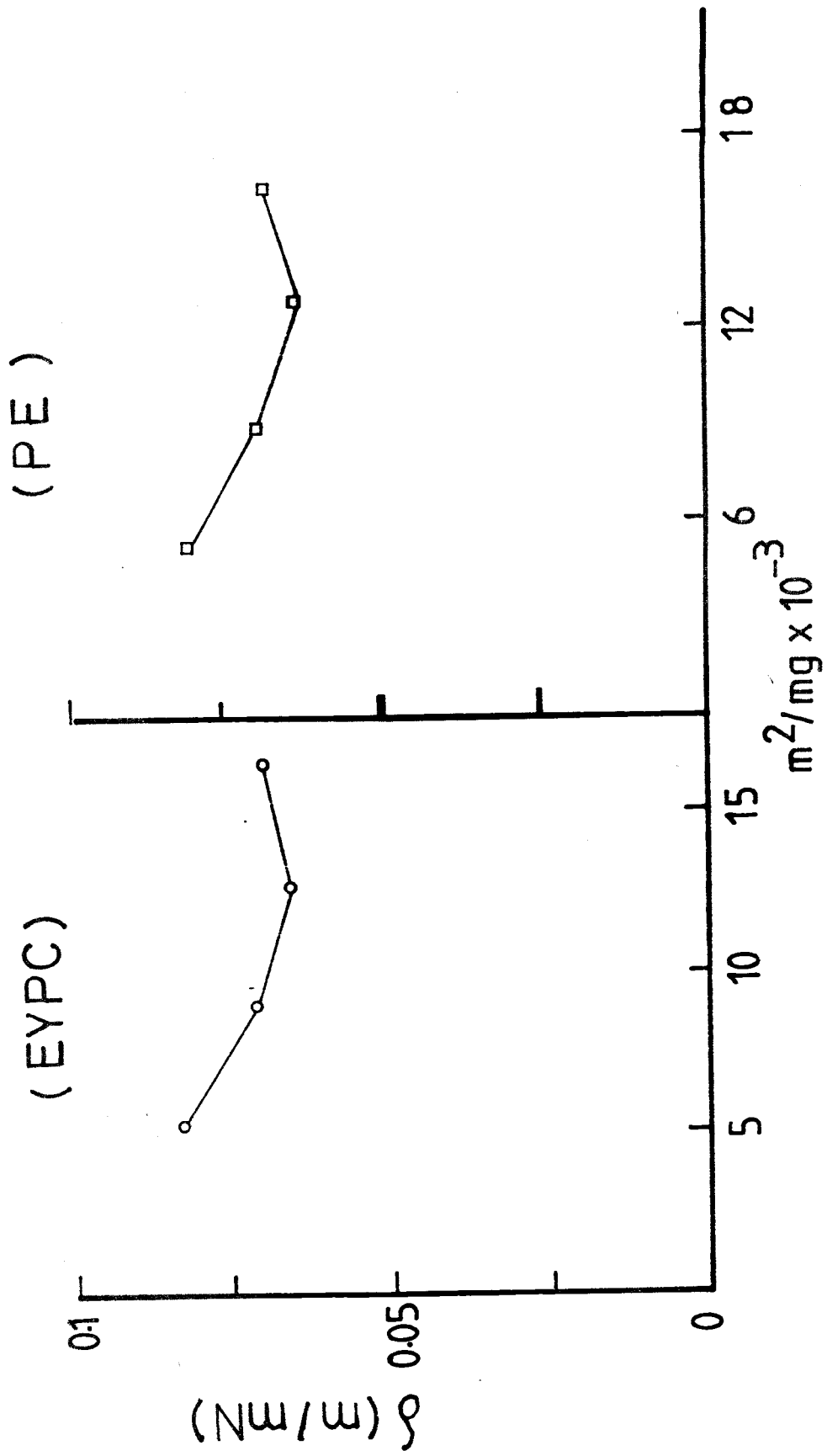
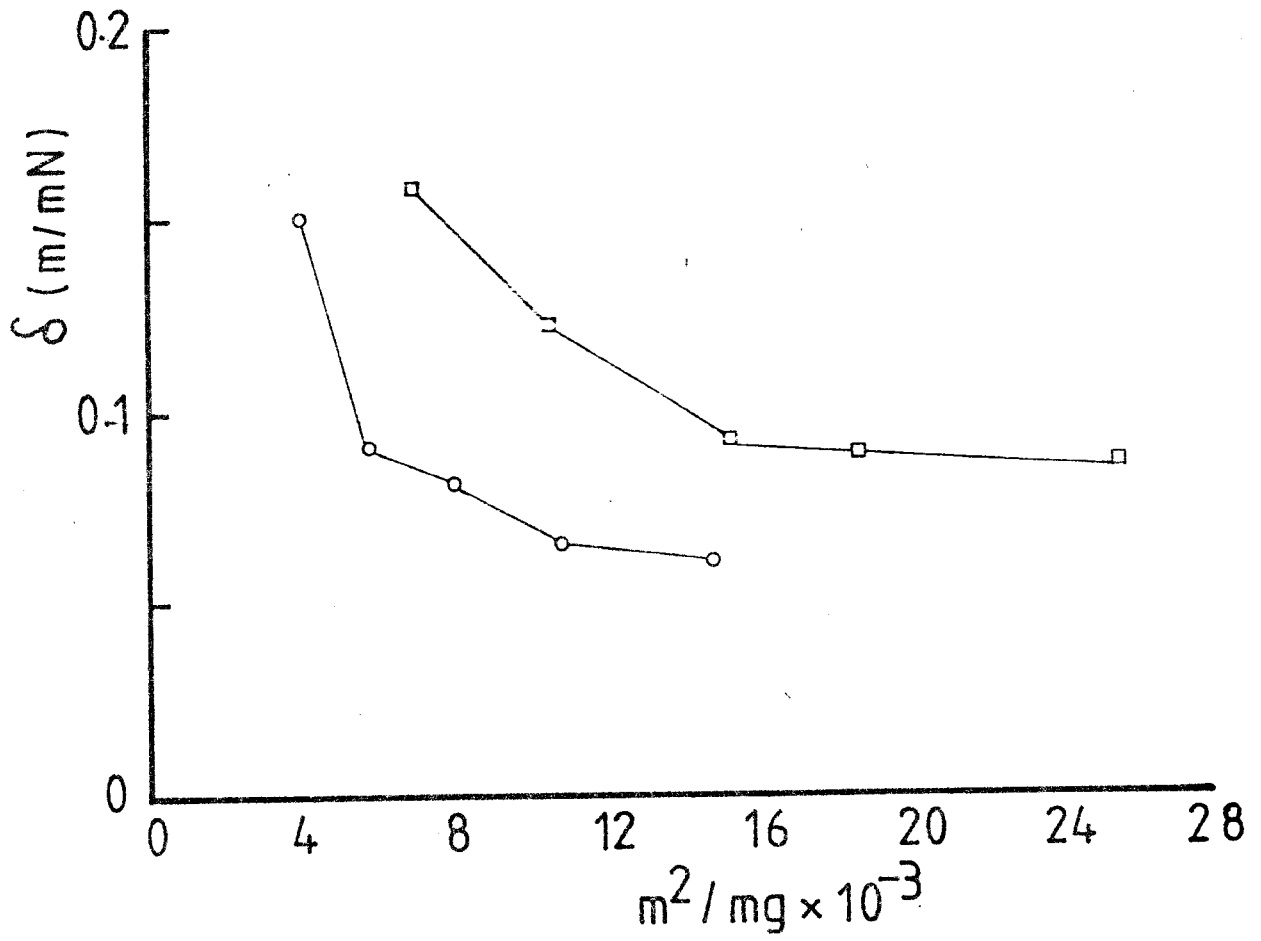


Fig. 5.14.b

Cholesterol



face pressure corresponding to the minima in the value of  $\delta$  showed a wide range of between 6 and 16 m/mN for PE and EYPC. As expected, these values increased as the VSG concentration was increased.

The minimum lateral compressibility values for the cholesterol-VSG interaction and the corresponding values for surface area per molecule of VSG are shown in Figure 5.14(b). These minima were exhibited when optimum quantities (0.1 to 0.25 mg) of VSG were used in these mixed monolayers. If quantities higher than 0.25 mg of VSG were used the minimum ( $\delta$ ) value was not clearly shown in the plot of the coefficient of lateral compressibility against the surface concentration of antigen. On the other hand, the use of concentrations of VSG lower than 0.1 mg, though permitting the calculation of minimum ( $\delta$ ) values, showed great variability even for the same VSG concentration. In contrast to the observation in the experiments with phospholipids, the surface concentration of VSG in the cholesterol monolayers showed minima located almost at the beginning of the curve. This may be interpreted as due to the complete saturation of the available area by VSG. The minima occur at a surface pressure of 7 to 9 m/m (from Figure 5.8(a)). The area of VSG inserted into lipid monolayers equivalent to the minimum value of  $\delta$  can be derived by transforming  $\text{m}^2/\text{mg}$  into  $\text{\AA}^2/\text{molecule}$ . This operation can be performed by multiplying the observed area ( $\text{m}^2/\text{mg}$ ) by a conversion factor of 10459 ( $\text{\AA}^2/\text{molecule}$ ). The surface areas per molecule of VSG inserted in the monolayer obtained by this method for PE and EYPC range in value between 120 and 150  $\text{\AA}^2/\text{molecule}$  at  $\delta$  values 0.05 to 0.06 m/mN. The number of equivalent amino acid residues inserted could be calculated by dividing the surface area per molecule of VSG

by  $15 \text{ \AA}^2$ . The average values are shown in Table 1(b).

The surface area for VSG molecule inserted into the cholesterol monolayer shows a much wider range of 84 to  $160 \text{ \AA}^2$ /molecule; and the equivalent number of amino acid residues inserted are 6 to 11 per protein molecule.

#### 5.4.4 The relative increase in area (R.I.A.)

An alternative method for calculating VSG surface area inserted into a lipid monolayer is the relative increase in area (RIA). RIA is defined as the increase in surface area per lipid molecule contributed by VSG at the same surface pressure as the lipid monolayer alone. From the force area curves for lipid alone and in presence of VSG, this difference was measured at a surface pressure of 10, 15 and  $20 \text{ mNm}^{-1}$ . The plot of the relative increase in area against the mole fraction of VSG was a straight line for PE and EYPC (0.18 to 0.5 mol fraction). The linearity for cholesterol monolayers, however, was more restricted, 0.006 to 0.03 mol fraction (Figure 5.15). The slope of each straight line was taken as the surface area occupied per VSG molecule and in Table 2 these calculations are summarised. Also, the effect of surface pressure in reducing the area occupied by VSG is shown as a percentage reduction in parentheses. The number of amino acid residues was calculated from the area per molecule at a surface pressure of  $10 \text{ mNm}^{-1}$  and these are also shown in Table 1(b).

#### 5.4.5 Miscibility within the film-forming molecules

I have adopted a very similar approach for estimating the surface area of VSG inserted in the lipid monolayer to that of Szabo & Brockman (1978). Although these authors did not use a lipid-protein



**Fig. 5.15**

**Relative increase** in area (RIA) is defined as the increase in **surface area per** molecule of lipid contributed by VSG at the **same surface** pressure as the lipid monolayer alone. From lipid **force-area** curves and lipid-VSG force-area curves RIA was measured as follows:

Cholesterol at (O) 10, ( $\Delta$ ) 15 and ( $\bullet$ ) 20 mN/m.

Phosphatidyl ethanol<sup>m</sup>amine at ( $\square$ ) 10, (X) 15 and ( $\Delta$ )

20 mN/m and phosphatidyl choline at ( $\square$ ) 10, (X) 15 and ( $\Delta$ ) 20 mN/m.

Fig. 15

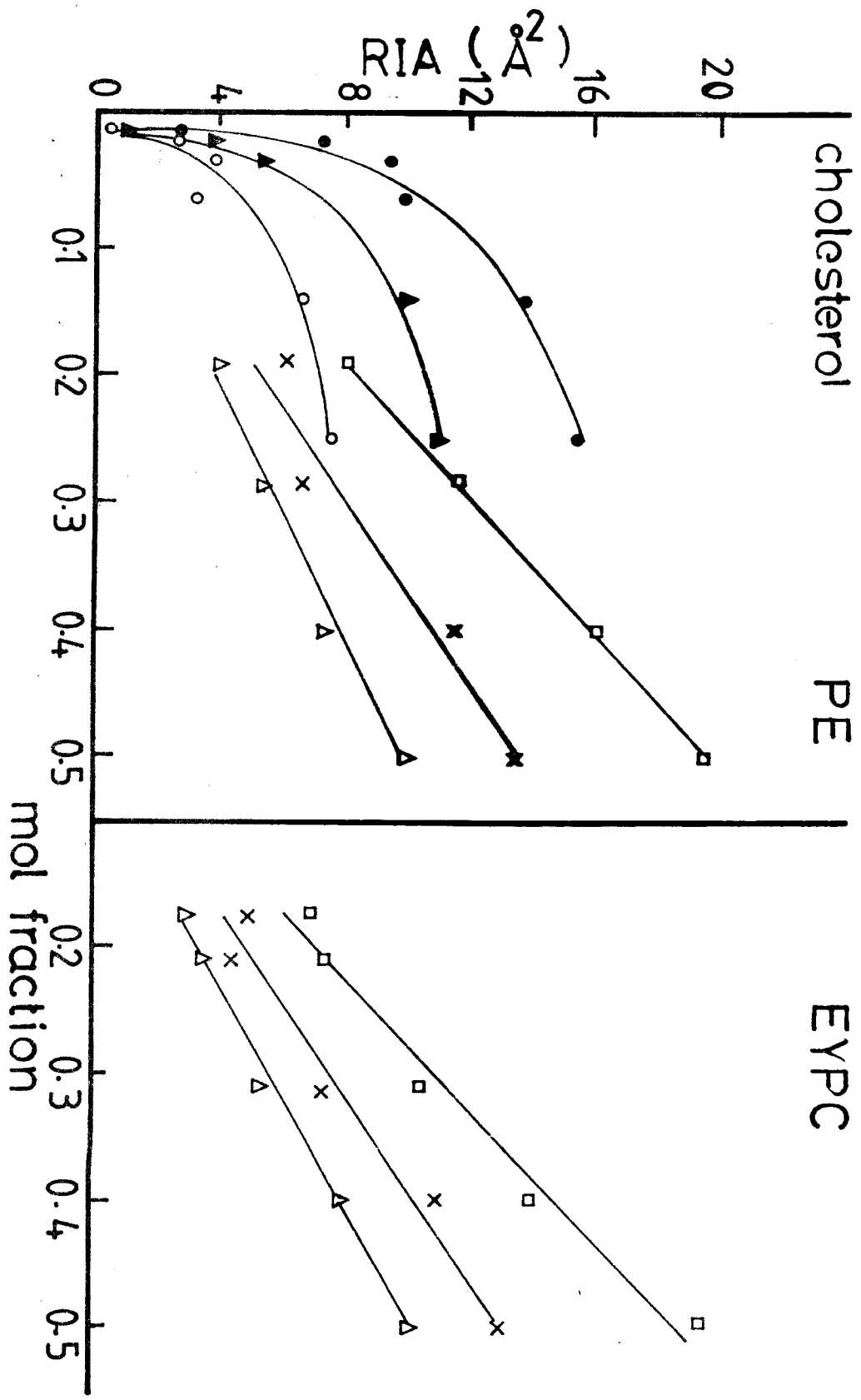


Table 2. Relative increase in area

Lipids	Relative increase area ( $\text{\AA}^2/\text{molecule}$ )			
	( mN/m:	10	15	20 )
CHL		96.8	85.9 (11%)	36 (63%)
PE		36.4	25.7 (29%)	22.2 (39%)
EYPC		38.5	32.7 (15%)	23.7 (38%)

Calculation of the relative increase area (RIA) for each VSG mole fraction is indicated in legend to Figure 5.15. The slope of the linear part of the plot RIA versus VSG mole fraction was calculated for surface pressures of 10 mN/m, 15 mN/m and 20 mN/m. The percentage values into brackets show how the original area at 10 mN/m is reduced by increasing the surface pressure.

system, several of the arguments that they applied to the triolein-cholesteryl oleate system are valid for a lipid-protein system. First of all, the requisite of miscibility (see section 6.1) is fulfilled by lipids and VSG at the air-water interface, thus the expansion of the lipid  $\pi$  - A curves shown in Figures 5.6, 5.1b and 5.8a is due to the presence of VSG. The  $\pi$  - A isotherms in presence of VSG indicates that  $\pi$  is a continuous function of the film area, which indicates that the spread film is homogenous (van Deenen et al., 1962; Gershfeld, 1974; Cornell et al., 1979). Furthermore the variability of the critical surface pressure according to the lipid-VSG ratio (Figure 5.16a) can be interpreted as the result of miscibility. Another indirect piece of evidence is that VSG has a certain mobility on the external parasite surface as detected by Barry (1979) who demonstrated the "capping" of VSG. Secondly, the criterion of the critical surface pressure, which is the point at which VSG is ejected from the monolayer, can be estimated from  $\pi$ -A curves.

The last criterion of equilibrium between lipid and antigen at the interface is fulfilled by the lipid-VSG  $\pi$ -A curves. Thus, compression and expansion are reversible indicating that VSG molecules remained adsorbed. Therefore, for such a miscible system at equilibrium, a plot of the negative  $\log_{10}$  of the mole fraction of VSG versus critical pressure should be linear for values of the mole fraction over which the activity coefficient of the component is constant (Smaby & Brockman, 1978). The slope of such a line should be

$$2.303 RT/A_c \dots\dots\dots (5.16)$$

$A_c$  is the molecular area of VSG at its point of ejection from the monolayer. R is the gas constant, and T is the absolute temperature

Fig. 5.16a

Determination of **critical** surface pressure ( $\Delta\pi_{\text{critical}}$ ).  $\Delta\pi_{\text{critical}}$  is defined as the **total** surface pressure at the discontinuity of the plot  $\Delta\pi$  versus **increased** surface pressure ( $\pi_{\text{inc}}$ ).  $\pi_{\text{inc}}$  is the total surface **presssure** of VSG and lipid determined from force-area curves.  $\Delta\pi$  is the **difference** between the surface pressure of the VSG-lipid **monolayer** and the surface pressure of lipid monolayer measured at the **same** area per molecule of lipid (equation 5.1). **Cholesterol-VSG** interactions were determined at the mol ratio of **cholesterol:VSG** (0) 1:15, ( $\square$ ) 1:30, ( $\bullet$ ) 1:6 and ( $\Delta$ ) 1:3. Phosphatidyl **ethanolamine:VSG** (x) 1:4.5 and ( $\blacksquare$ ) 1:1. Phosphatidyl **choline:VSG** ( $\Delta$ ) 1:4:4 and ( $\circ$ ) 2:3.

Fig. 5.16b

Plot of  $\Delta\pi_{\text{critical}}$  versus the negative logarithm of the mol fraction (lipid/VSG) for (0) cholesterol, ( $\Delta$ ) phosphatidyl choline and ( $\square$ ) phosphatidyl ethanolamine.

Fig. 5.16.a

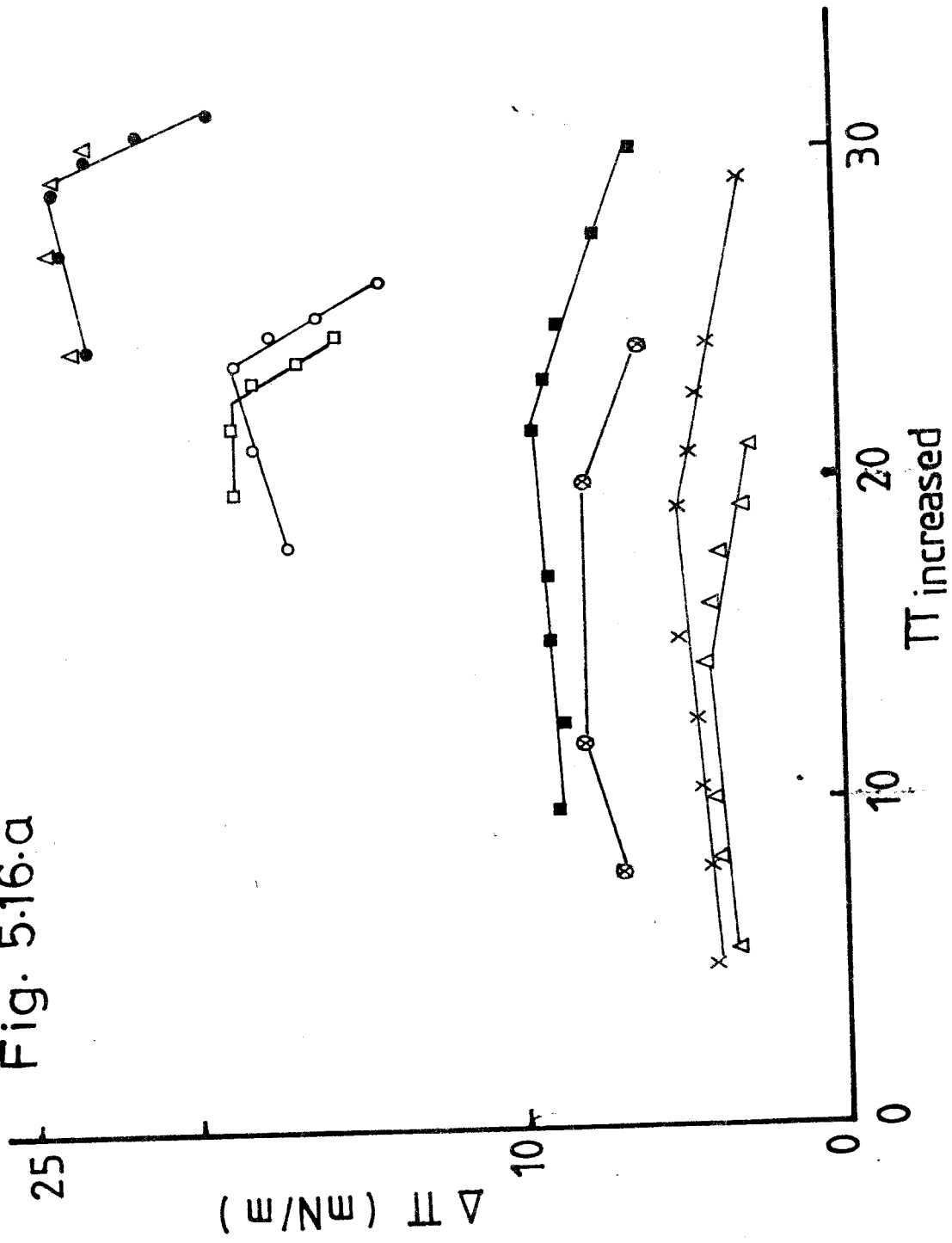
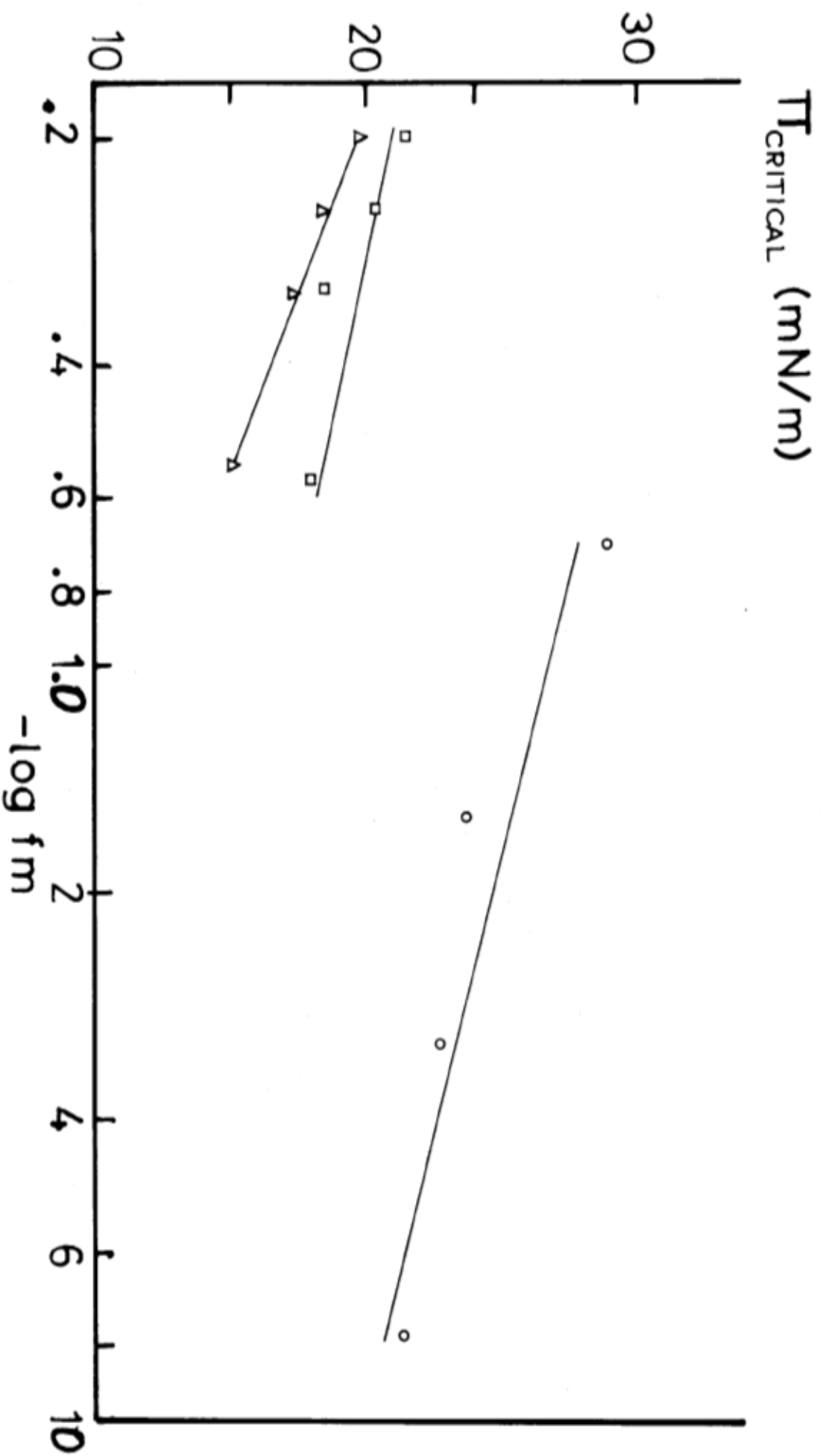


Fig. 5.16.b



(°K). The value of the critical surface pressure ( $\pi_{\text{critical}}$ ) for interaction of VSG and lipid at the interface could be obtained from the plot of  $\Delta\pi$  versus increased surface pressure ( $\pi_{\text{inc}}$ ).  $\Delta\pi$  was defined at the beginning of this Chapter in section 5.1.1;  $\pi_{\text{inc}}$  is the total surface pressure ( $\pi_{\text{Lipid}} + \Delta\pi$ ) due to VSG for the same lipid molecular area.

The graphs (Figure 5.16a) show that a plot of  $\Delta\pi_{\text{VSG}}$  versus  $\pi_{\text{inc}}$  exhibits a discontinuity at a certain  $\pi_{\text{inc}}$ . It could therefore be assumed that such discontinuities are due to the exclusion of VSG, and that the total surface pressure ( $\pi_{\text{inc}}$ ) at which the process occurs is the critical surface pressure ( $\Delta\pi_{\text{critical}}$ ). Figure 5.16b shows how  $\Delta\pi_{\text{critical}}$  increases as VSG concentration is raised. For phospholipids saturation is not apparent even at a molar ratio of 1:1. For CHL,  $\Delta\pi_{\text{critical}}$  exhibits higher values than this even at a molar ratio of 1:156 which means 40 times less antigen is needed for the same number of lipid molecules as compared to phospholipids. Also saturation is suggested by the data at a molar ratio of 1:6.

The equation (5.16) suggested by Smaby & Brockman (1978) was applied to the slopes computed from the data of Figure 5.16b. Hence, the surface area per molecule of VSG ( $A_c$ ) inserted into the lipid monolayer were as follows ( $\text{\AA}^2/\text{molecule}$ ):  $161 \pm 1$  for cholesterol monolayers;  $130 \pm 3$  for PE monolayer and  $90 \pm 2$  for EYPC monolayer.

#### 5.4.6 Interpretation of surface dipole moment for lipid monolayers in presence of VSG

When a lipid monolayer is spread on a clean water surface the water dipoles at the surface are re-orientated around the dipoles of the film-forming molecules. The relationship between surface potential and dipole moment is established by the equation, excluding



double layer effects

$$\Delta v = 4 \pi n \mu_{\perp} \quad \dots\dots\dots (5.17)$$

n is the number of dipoles per area according to Davies & Rideal (1963, pp 72). The equation (5.17) likens the film to a parallel plate condenser. n is the number of dipoles per unit area (cm<sup>2</sup>);  $\mu_{\perp}$  is the surface dipole moment.  $\mu_{\perp}$  is assumed to be due to an intrinsic moment ( $\bar{\mu}$ ) making some angle with respect to the monolayer director normal to the interface.

$$\mu_{\perp} = \bar{\mu} \cos \theta \quad \dots\dots\dots (5.18)$$

So, for the film-forming molecules, the surface dipole moment ( $\mu_{\perp}$ ) is the overall dipole moment in a direction perpendicular to the interface, resulting from:

$$\mu_{\perp} = \mu_{\perp 1} + \mu_{\perp 2} + \mu_{\perp 3}$$

where  $\mu_{\perp 1}$  is the contribution from the oriented water molecules,  $\mu_{\perp 2}$  from the polar head group, and  $\mu_{\perp 3}$  from the hydrocarbon chains. (See schematic representation in Figure 5.18).

Although equation (5.17) has certain limitations as discussed by Gaines (1966, pp 189), it reflects in general the average of the surface dipole moment which for an un-ionised monolayer becomes,

$$\mu_{\perp} = \Delta v A / 12 \pi \quad (\text{milli Debye units, MD}) \quad \dots\dots (5.19)$$

A in Å<sup>2</sup> per molecule; Δv in millivolts.

When monolayers are composed of ionic molecules their behaviour is different from those of neutral films. The balance between intermolecular forces in the film and the forces between the subphase are

film-forming molecules which exists in a neutral film are affected when the molecules comprising the monolayer are charged. The factors affecting this balance are:

- (i) the direct electrostatic repulsion or attraction which is operating within the film, and between the film and subphase;
- (ii) the presence of counter-ions introduced by the dissociation of the ionic compound, when it is spread, which maintains the electrical neutrality of the entire system.

The presence of these counter-ions and the charged insoluble film establish an ionic double layer. Models of the double layer are shown in Figure 5.17, and are further discussed by Davies & Rideal (1963, pp 75), Aveyard & Haydon (1973, Chapter 2) and Moore (1978, pp 510). The former authors applied the modified model of Gouy & Chapman to ionised monolayers. In this model the relationship between surface potential and dipole moments includes the electrostatic potential ( $\Psi$ ) due to the contribution of ions, and was summarised by Davies & Rideal (1963) as:

$$\Delta v = 4\pi n\mu l + \Psi_{AB} \dots\dots\dots (5.20)$$

The first term is the conventional expression for the surface dipole moment and  $\Psi_{AB}$  represents the potential difference between the surface (A) and the bulk of the subphase (B);  $\Psi_{AB}$  may be substituted by  $\Psi_0$  which is the potential difference at the interface.

$$\Psi_0 = \frac{2KT}{e} \sinh^{-1} \frac{\epsilon}{(2C_i DKT/\pi)^{\frac{1}{2}}} \dots\dots\dots (5.21)$$

$C_i$  is the total univalent electrolyte concentration in moles per litre.

$K$  is the Boltzman constant

$T$  is the absolute temperature

$e$  is the electronic charge

$D$  is the dielectric constant of the medium (for water  $D = 80$ )

$\epsilon$  is the charge density per  $\text{cm}^2$ .

At  $20^\circ\text{C}$  the equation (5.21) can be simplified to

$$\psi_0 = 50.4 \sinh^{-1} \left( \frac{134}{A c_i^{1/2}} \right) \dots \dots \dots (5.22)$$

where  $C_i$  is the molar concentration of salt in the subphase,  $A$  is the area per charged group and  $\psi_0$  is in millivolts.

It is interesting to mention the extension of the applicability of double layer theory to the study of the screening effects of both monovalent and divalent ions on the surface potential of charged phospholipid bilayers inferred from conductance measurements by McLaughlin et al. (1971).

The lipid monolayers used in these experiments had not net charge (i.e. were isoelectric) and  $\mu_l$  may be calculated using equation (5.19) throughout the range of compression of the lipid monolayer; however, at high surface area per molecule it was not possible because of fluctuations in  $\Delta v$ . Evidently, the VSG contribution to the surface dipole moment is minimal for phospholipid monolayers as shown in Figure 5.17. At large surface areas per phospholipid the  $\mu_l$  values were not very different from those observed in presence of VSG. Owing to the characteristics of condensed films  $\mu_l$  becomes highly variable at higher surface area per cholesterol molecules than  $50 \text{ \AA}^2$ . The addition of VSG to that film at high surface area practically abolished the fluctuations in mV. Its contribution to the value of  $\mu_l$  is shown in Figure 5.17. VSG contributes to the resultant surface dipole moment at high surface areas, but the contribution is diminished gradually as the area per molecule is reduced. It is possible

Fig. 5.17

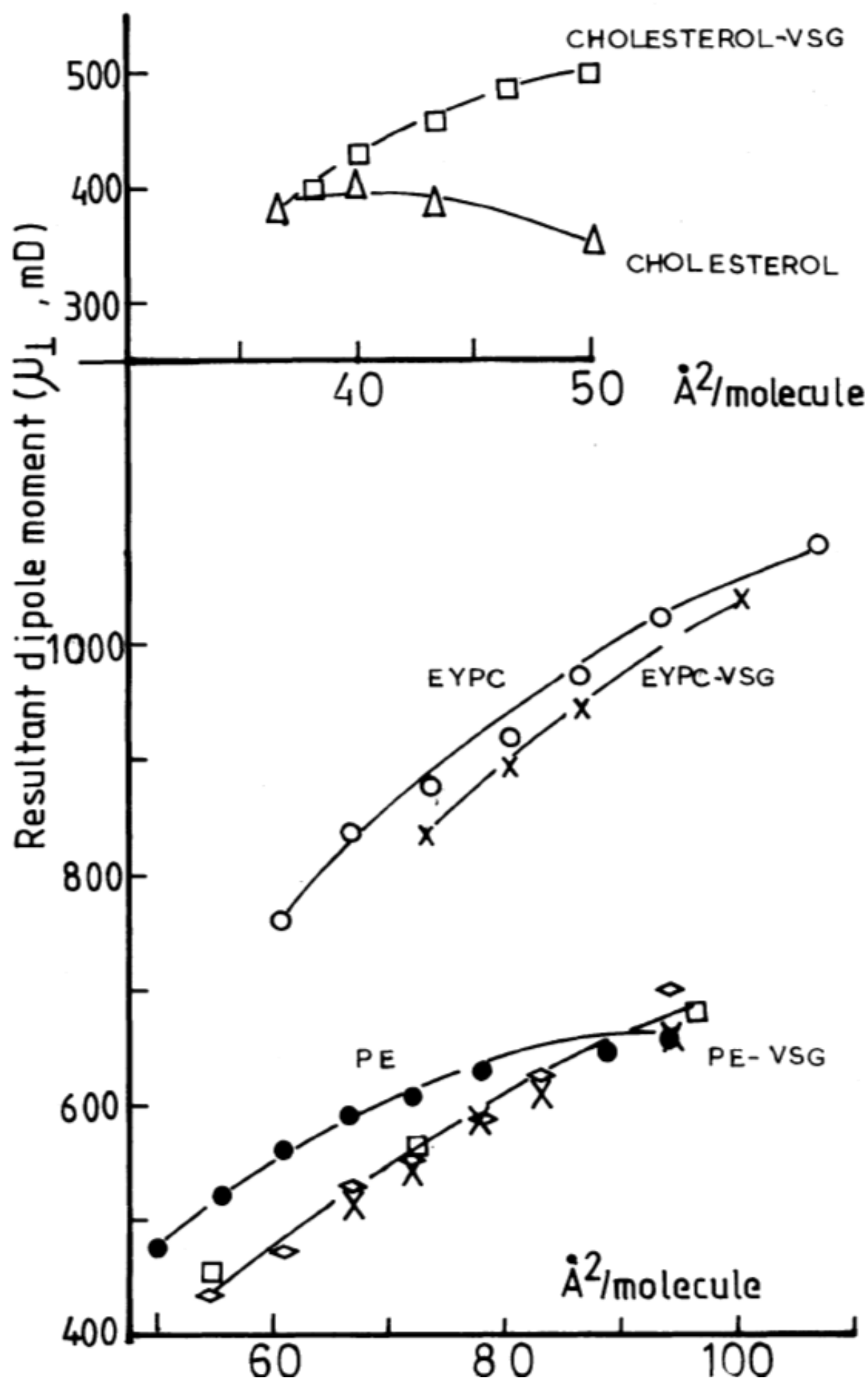
Resultant dipole moment ( $\mu$ ) was calculated using equation (5.19), see Table 5.3. The monolayer composition was as follows:

Cholesterol:VSG mol ratio 1:6.

Phosphatidyl choline:VSG mol ratio 1.5:1.

Phosphatidyl ethanolamine:VSG mol ratio ( $\diamond$ ) 1:1, ( $\square$ ) 2:1 and (x) 1.5:1.

Fig. 5.17



that some amino acid side chains reach the air boundary contributing to  $\mu_3$ ; and the reduction of  $\mu_1$  to similar values at the limiting area for cholesterol may indicate the ejection of VSG or its hydrophobic side chain from the cholesterol monolayer. Ergosterol films gave similar results in the presence of VSG.

The reduction of the area per molecule of lipid occurs together with an increase in surface potential equivalent to the reduction of the surface dipole moment. The increase in  $\Delta v$  reaches a constant value in the proximity of the limiting area ( $\sim 40 \text{ \AA}^2$  per sterol molecule).

Thus, the surface dipole moment was calculated for the lipid monolayers alone, and in the presence of antigen, at the corresponding area per molecule where  $\Delta v$  showed constant values. The  $\mu_1$  values shown in Table 3 were calculated for a VSG:sterol ratio of 1:6, and a VSG:phospholipid ratio of 1:6. For cholesterol monolayers the range of the ratio of VSG:CHL between 1:6 and 1:31 showed values for surface dipole moment within the average value given in Table 3. For PE and EYPC, the average VSG:phospholipid ratios from 1:4 to 1:1 yield  $\mu_1$  values similar to the average value shown in Table 3.

Table 3 Contribution of VSG to resultant surface dipole moment ( $\mu_l$ ) of lipids.

Lipids	$\mu_l$ (mD)	
	Without VSG	With VSG
SBPC	620 $\pm$ 40	577 $\pm$ 30
DMPC	698 $\pm$ 43	706 $\pm$ 21
DOPC	767 $\pm$ ND <sup>a</sup>	652 $\pm$ ND <sup>a</sup>
DPPC	523 $\pm$ 10	540 $\pm$ 50
EYPC	746 $\pm$ 80	698 $\pm$ 100
CHL	411 $\pm$ 5	400 $\pm$ 27
ERG	517 $\pm$ 15	538 $\pm$ 46

(SBPC, soybean phosphatidyl choline; DMPC, dimyristoyl phosphatidyl choline; DOPC, dioleoyl phosphatidyl choline; DPPC, dipalmitoyl phosphatidyl choline; EYPC, egg yolk phosphatidyl choline; CHL, cholesterol; ERG, ergosterol).

Equation (5.19) can be rewritten as

$$\mu_l = 0.0265 \times mV \times \overset{02}{A^2}$$

A molar ratio of VSG : sterols of 1 : 6 was used. For phospholipids it was VSG : phospholipid 1 : 4.

The composition of the subphase is described in the Material and Methods Section; pH was 6.8.

a) This value is the average of 2 determinations, the other values are averages of 3 determinations each.

## 5.5 Discussion

### 5.5.1 Some properties of phospholipids and sterols at the air-water interface

Although there is a vast literature describing the study of the properties of lipid monolayers at the air-water interface, it was considered important to establish a system of reference for VSG. From the force-area ( $\pi$ -A) and surface potential-area ( $\Delta V$ -A) curves for phosphatidylcholine, a limiting surface area of  $60\text{\AA}^2$  per molecule was calculated. This is in agreement with that reported in the literature (Demel & De Kruyft, 1976; Barenholz, 1980). For natural phosphatidylcholine, however, this value as reported from one laboratory to another varies partly because EYPC has a variable composition depending on diet fed to the hens consisting mainly of 1-palmitoyl-2-oleoyl phosphatidylcholine mixed with other PCs containing different fatty acid substituents (Huang, 1977; Ladbroke & Chapman, 1969; Klein, 1970b). The other contributory factor is the difficulty in measuring the collapse pressure accurately. Egg yolk phosphatidylcholine possesses a large proportion of long saturated hydrocarbon chains and has a high collapse point thereby making the measurement technically difficult (Müller-Landau & Cadenhead, 1979, Part 1). Thus the limiting surface area for phospholipids described in the literature has sometimes been determined at a surface pressure of  $30\text{ mNm}^{-1}$ , which is below the collapse pressure (Demel et al., 1972).

The effect of unsaturation on the shape of the  $\pi$ -A curve is demonstrated by comparing EYPC (Fig. 5.1), SPC (Fig. 5.2) and DOPC (Fig. 5.3), all of which contained unsaturated fatty acids (i.e. C18:0/C18:1, C18:2/C18:2 and C18:1/C18:1 respectively). Amongst these, only DOPC



exhibited a more compressible  $\pi$ -A curve, possibly because it contained only one molecular species, whilst the other two phospholipids are mixed as regards species. These observations are supported by Demel et al. (1972) who have demonstrated that the limiting area for 1,2-distearoyl phosphatidylcholine was  $42\text{\AA}^2$ , whilst for 1-stearoyl-2-oleoyl phosphatidylcholine the value was  $61\text{\AA}^2$ . Furthermore, the introduction of multiple double bonds, i.e. polyunsaturation, into the fatty acid chains increases the molecular area to  $76\text{\AA}^2$ . The shape of the  $\pi$ -A curves for unsaturated phospholipids contrasts with that of either DSPC (C18:0/C18:0) or DPPC (C16:0/C16:0) both of which are completely saturated. These latter phospholipids form condensed monolayers at room temperature (See Fig. 5.5).

Another important factor which governs the lipid physical state at the air-water interface is the length of the saturated hydrocarbon chains of the phospholipids. Phospholipids containing C10:0/C10:0, C12:0/C12:0 and C14:0/C14:0 show  $\pi$ -A isotherms corresponding to expanded monolayers; but by increasing the number of methylene ( $-\text{CH}_2-$ ) groups in the hydrocarbon chain from C16:0/C16:0 to C22:0/C22:0, it is possible to observe the transition from expanded to condensed monolayers at room temperature (Phillips, 1972). The elegant work of Phillips & Chapman (1968) demonstrated for DPPC that there is a correlation between temperature and the physical state of the lipid film. A monolayer of DPPC could exist in all the classical monolayer states when the experimental temperatures are varied above and below its transition temperature (Baret et al. (1982). The polar head groups have been found to play an important part in these phase transitions. Hence eight phases were observed for insoluble fatty acid monolayers in a temperature range between  $3^\circ$  and  $40^\circ\text{C}$  (Baret et al., 1982).

Sterol monolayers showed the characteristic force-area curves for condensed monolayers (Figs. 5.8a and 5.9). The difference in surface area between an initial low surface pressure ( $\sim 2 \text{ mNm}^{-1}$ ) and that at the attainment of a high surface pressure ( $20 \text{ mNm}^{-1}$ ) is approximately  $3\text{\AA}^2$ . For an EYPC monolayer the surface area for this range of surface pressure is approximately  $25\text{\AA}^2$ .

#### 5.5.2 Behaviour of VSG in monolayers of phospholipids and sterols

The addition of VSG to phospholipid monolayers produced a displacement of the lipid force-area curve and a less pronounced displacement of the surface potential-area curves. In these experiments VSG was spread at the interface containing the phospholipid monolayer, so that the  $\pi$ -A curve for lipid-VSG may be compared quantitatively with that for lipid alone. The increase in surface pressure at the same area per lipid molecule due to the presence of VSG ( $\Delta\pi_{\text{VSG}}$ , see Sections 5.1.12) can be ascribed to the insertion of either a part of, or the entire molecule of VSG into the lipid film. This value for the change in  $\Delta\pi_{\text{VSG}}$  reached a maximum value (Fig. 5.16a) which was taken to represent the critical surface pressure for the VSG-lipid mixed monolayer. The force-area curves for various phospholipids in the presence of VSG were very similar. Nevertheless,  $\Delta\pi_{\text{critical}}$  for dipalmitoyl phosphatidylcholine was found to be higher than for other phosphatidylcholines (Table 4). Thus, with the exception of DPPC, the difference between  $\Delta\pi_{\text{critical}}$  for each lecithin was less than  $\pm 2 \text{ mNm}^{-1}$ .

The interaction of VSG with sphingomyelin was extremely weak and gave the lowest  $\Delta\pi_{\text{critical}}$  values. As a consequence, these values have not been shown in Table 4 because  $\Delta\pi_{\text{VSG}}$  was too low to permit such calculations. Hence sphingomyelin monolayers may be taken as a negative

Table 5.4 Critical surface pressure for the interaction of VSG with different lipid monolayers

<u>Lipids</u>	<u><math>\Delta\pi_{\text{critical}}</math></u>	<u><math>\Delta\pi_{\text{net}}</math></u>
DPPC	20.6	10.6
DOPC	14	4
DMPC	23.4	7.4
SBPC	15	5
EYPC	14.2	4.2
PE	21	5
CHL	29	24
ERG	22	20

For lipid abbreviation see **Table 3**.

The critical surface pressure ( $\Delta\pi_{\text{critical}}$ ) is defined as the total surface pressure at the discontinuity of the plot  $\Delta\pi$  versus  $\pi_{\text{inc}}$  (see Fig. 5.16a). The total surface pressure, or increased surface pressure ( $\pi_{\text{inc}}$ ) is the sum of  $\pi_{\text{lipid}}$  and the surface pressure due to YSG ( $\Delta\pi_{\text{VSG}}$ ) measured at the same area per molecule of lipid.  $\pi_{\text{inc}}$  was determined from force area curves for lipid monolayers in presence of YSE. The net surface pressure ( $\Delta\pi_{\text{net}}$ ) is the surface pressure due to YSG at the point where  $\Delta\pi_{\text{critical}}$  occurs.

Details of these procedures are given in **Section 5.4.5**.

The antigen was added at a molar ratio of YSG:lipid of 1:4, or 1:6, with the subphase at pH 6.8.

control showing no significant interaction with VSG. From the results shown in Fig. 5.7, it could be inferred that there is no mixing between VSG and SPH molecules; and, significantly, at near to zero surface pressure, VSG was not adsorbed at the interface. The ability of VSG to adsorb at the air-water interface has already been demonstrated (Section 5.3). The results with sphingomyelin monolayers, therefore, suggest the possibility that there exists a functional group in the sphingomyelin molecule which repels the hydrophobic residues of VSG. This chemical group could be the spingosine chain; the polar phosphorylcholine group being discounted since it is common to both sphingomyelin and phosphatidylcholines. Colacicco (1970) observed a similar result of non-penetration of sphingomyelin monolayers by the  $\gamma$ -globulin from rabbit; and he proposed a mechanism of 'binding-inhibited penetration' for such system. According to this mechanism, the protein binds to the lipid hydrophilic groups which extend into the subphase; and the bound protein blocks the routes of access to the interface, thus the resultant interfacial  $\pi$ -A isotherm is not altered. Although there has been no further evidence in support of this mechanism, it is considered here because of the similarity of the interaction of VSG with sphingomyelin monolayers. Furthermore, this is relevant in the light of new information for the structural arrangements of sphingomyelin and phosphatidylcholine at the air-water interface discussed below.

The differences between sphingomyelin and lecithin at the interfacial region are very considerable as shown in Fig. 5.18. For phosphatidylcholine the interface includes, Carbon atoms 1, 2 and 3 of the glycerol backbone, and the components of the two ester bonds linking

the acyl groups (Huang, 1976; Seelig, 1980). In sphingomyelin, this region contains the amide bond and the primary amino group on Carbon atom 2 in addition to the hydroxyl group on Carbon atom 3, and also possibly the trans-double bond between Carbon atoms 4 and 5 of sphingosine (Barenholz & Thompson, 1980). Hence the difference between sphingomyelin and lecithin is that sphingomyelin, at the interfacial region, exposes the hydroxyl group and the amide groups both of which are important hydrogen bond donors. Other hydrogen bond donors in this region are the ester carbonyl groups of phosphatidyl choline. At this interfacial region the hydrogen bonds formed by the donor groups of these lipids could be expected to be very strong. Hence the hydrogen bonds between them and protein acceptors will be stronger than such bonds formed in an aqueous medium (Huang, 1977).

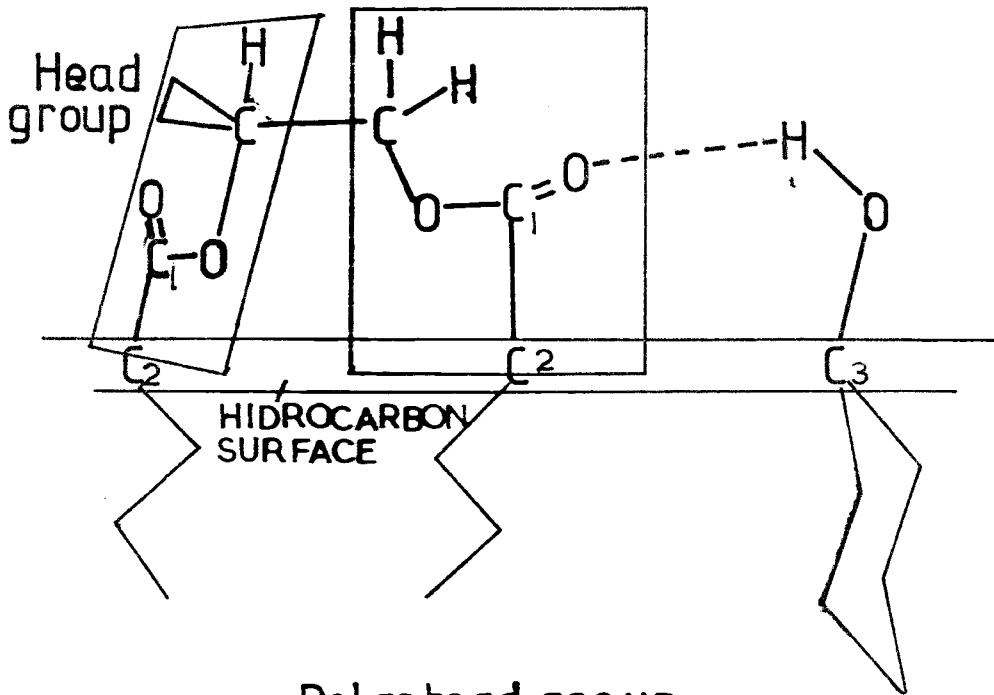
The concentration of VSG used in these experiments was low enough to avoid the formation of dimers (Auffret & Turner, 1981). Increasing the pH from 6.8 to 8.0 (VSG<sub>151</sub> isoelectric point 6.8) could be expected to increase the number of monomers thus increasing the probability of interaction of VSG with sphingomyelin monolayers. In addition, there appears to be no restriction on this interaction through electrostatic forces as shown by the reduction in ionic strength from 0.157 $\mu$  to 0.011 $\mu$  which did not enhance the interaction (Section 5.1.7). Using radio-labelled antigen, however, it was demonstrated that VSG is adsorbed to sphingomyelin monolayers, thus suggesting that although adsorption occurs, VSG is unable to reach the hydrophobic sites of the phospholipid molecules. In view of the discussion above, this observation could be interpreted to mean that some interacting groups in VSG establish hydrogen bonds with sphingomyelin molecules thereby placing

Fig. 5.18

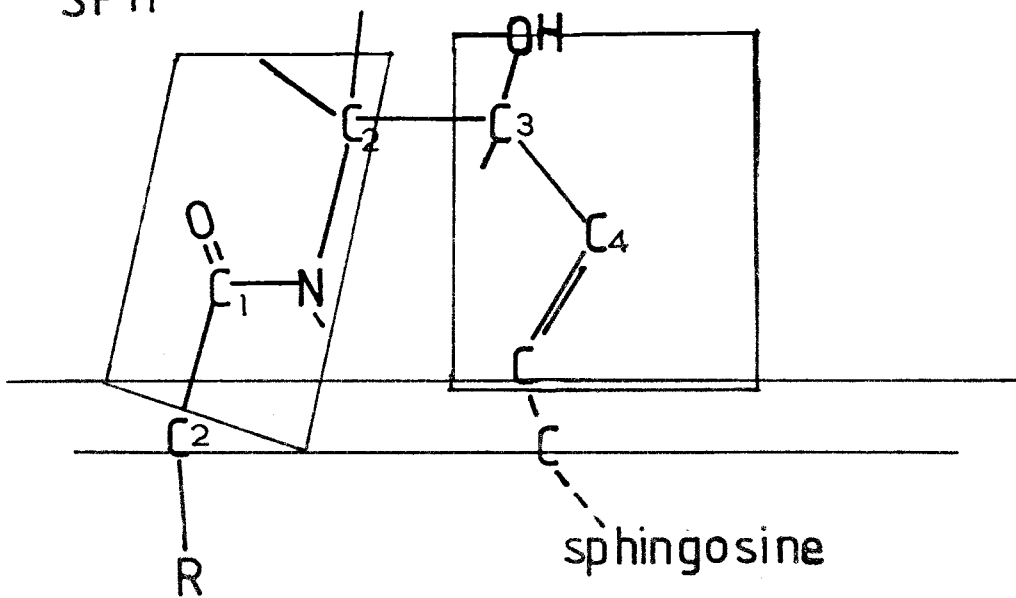
Schematic representation of the interface region of the bilayer composed of phosphatidyl choline and cholesterol. The planarity of the structural element  $-COC_1OC_2-$  is shown. The formation of the hydrogen bond between the cholesterol  $3\beta$ -hydroxyl group and the phospholipid carboxyl group is outlined by broken line. Sphingomyelin (SPH) exposed at the same interface as the amino group and the hydroxyl group which are hydrogen donors. After Huang (1977) and Barenholz & Thompson (1980).

Fig. 5.18

PC



SPH Polar head group



a spatial restriction on the hydrophobic groups on VSG which are thus prevented from penetrating the interface. Surface adsorption of protein molecules without penetration into a lipid film has been observed by Papahadjopoulos but he did not attempt to explain the mechanism of such an interaction (Papahadjopoulos, 1975).

*In contrast to the above system, the interaction of VSG with sterols was clearly stronger than with phospholipids.* It was observed (Fig. 5.12) that the available surface area of a cholesterol monolayer is practically saturated with VSG at a molar ratio of 1:5 (VSG: cholesterol). At similar VSG-phospholipid molar ratios, appreciable changes in surface pressure were observed, but the values of critical surface pressure for the VSG-cholesterol system are about four times greater than the average values for VSG-phospholipids (Table 4).

Although the interaction of VSG with ergosterol was much stronger than with phospholipids, it displayed a critical surface pressure for below that measured for cholesterol. Similar observations were also made in experiments of the penetration of ergosterol and cholesterol monolayers by VSG (Section 6.3).

Studies of the VSG-lipid interaction using surface potential versus area curves suggest a qualitative difference between the interaction of VSG with phospholipids and that with sterols (Figs. 5.8a, 5.1b and 5.6). Hence at large areas per cholesterol molecule ( $\sim 60\text{\AA}^2$ )  $\Delta V$  fluctuated considerably and could not be measured accurately. In the presence of VSG, however, a stable surface potential was obtained. When the mixed VSG-CHL monolayer was compressed to the limiting area of cholesterol ( $39\text{\AA}^2$ ), the  $\Delta V$  reached values ( $3.60 \pm 20$  mV) which were similar to those obtained for cholesterol at that area.

In phospholipid monolayers a stable surface potential could be measured until a high area per molecule ( $\sim 90\text{\AA}^2$ ) was reached (Fig. 5.1b).



The presence of VSG increased that value by approximately 30 mV; and when this film was compressed to almost the limiting area the surface potential decreased to values which were 20 mV below those obtained for the phospholipid alone. An attempt to assess the contribution of VSG to the surface potential of phospholipid monolayers was carried out by plotting the increment in the surface potential  $\delta(\Delta V)$  versus the area per lipid molecule. The increment in mV was taken as the difference between two subsequent values starting from the value at which  $\Delta V$  was stable.

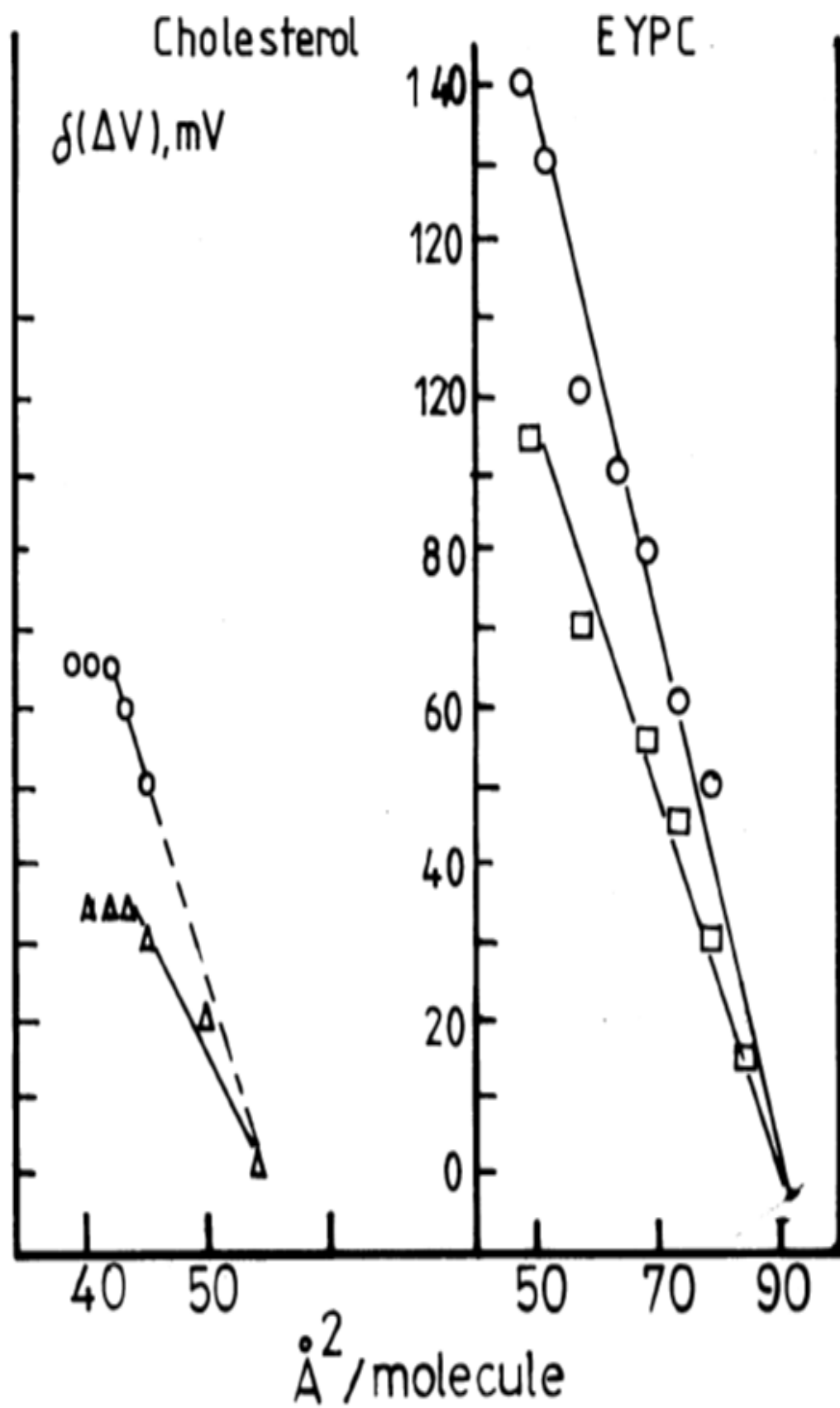
The plots of  $\delta(\Delta V)$  versus area for phosphatidylcholine and cholesterol are shown in Fig. 5.19. This treatment shows that during the interaction of the film-forming molecules (liquid phase) the increment in mV is directly proportional to the reduction in area per lipid molecule. This linearity was maintained in the presence of VSG, although the  $\delta(\Delta V)$  values were less than those measured for lipids alone. These observations argue in favour of miscibility between VSG and lipid molecules (see Gaines p. 281, 1966). A further explanation for the reduction in  $\delta(\Delta V)$  in the presence of VSG is discussed below.

From these results it can be deduced that VSG makes a significant contribution to the surface potential of cholesterol monolayers; but it only does so at high area per cholesterol molecule. In phospholipids, however, this contribution is considerably less, and leads in fact to negative values at areas very close to the limiting surface area of the phospholipid molecule. A detailed explanation of this observation cannot be given in terms of surface potential alone since the latter is a complex variable function of the number of dipoles per area, the dipole moments of molecules at the interface, the electrical double layer potential and ionic strength. It was found more convenient

Fig. 5.19

The linear plots of  $\delta(\Delta V)$  versus area per molecule of lipid are shown for the interaction of VSG with phosphatidyl choline and cholesterol.  $\delta(\Delta V)$  is the increase in surface potential starting from a known surface potential value at a designated surface area as the surface pressure is increased.

Fig. 5.19



to express these results in terms of surface dipole moments (Section 5.4.6). As shown in Fig. 5.17 the contribution of VSG to the surface dipole moment of phospholipids at large surface area per molecule is not large. Moreover, compressing the VSG-phospholipid film results in values below those for phospholipid alone at a surface area of  $70\text{\AA}^2$ . Whether this reduction in surface dipole moment is due to the exclusion of dipoles from the interface or to the perturbation of phospholipid polar groups of VSG is difficult to evaluate from the present data. On the one hand the possibility of the exclusion of phospholipid dipoles is not supported by the force-area curves; and on the other hand the possibility that at a high surface pressure ( $30\text{ mNm}^{-1}$ ) VSG could displace EYPC to the subphase seems improbable. The reason for this derives perhaps from the thermodynamics of the system since the compound having the highest equilibrium spreading pressure (phosphatidylcholine) will preferentially adsorb at the interface (Gershfeld & Pagano, 1972). On the other hand evidence from other monolayer systems shows that modifications in the polar head group have a profound influence on surface dipole moments. Thus ganglioside, a sphingolipid containing two to three sialosyl groups, contributes to a higher surface dipole moment than those containing one sialosyl group (Maggio, 1978).

From the results discussed above the preferential order of interaction of VSG with lipids is cholesterol  $\approx$  ERG  $\gg$  PE = PC > SPH. Apo A-I, a purified plasma lipoprotein, has been demonstrated as having a similar order of affinity for lipids (Camejo et al., 1968).  $A_1$ , a basic myelin protein, manifests a different pattern, however, the order of its affinity for lipids being: cerebroside sulphate > PS > PE > cholesterol > PC (London et al., 1974; Demel et al., 1973).

### 55.3 VSG alone at the air-water interface

These studies were aimed at determining the adsorption characteristics of VSG at the interface in the absence of lipids. The adsorption was measured as a change in surface pressure and surface potential. Comparison of the results from VSG spread on the water surface, and VSG injected beneath the surface into the bulk solution showed the adsorption to be less pronounced in the latter condition. This discrepancy could be ascribed to the amount of protein adsorbed at the interface, which may be different for both methods. The number of molecules adsorbed at the interface in the spreading technique is probably more than that due to diffusion from the bulk solution (Trurnit, 1960). This is probably because under these conditions complications arise due to: (i) unavoidable losses by adsorption onto the walls of the trough and (ii) the very long time taken for diffusion of all protein molecules to the interface (MacRitchie, 1978). The results for both techniques shown in Fig. 5.10a are consistent with the above interpretations. Hence the  $\pi$ -A isotherm for the surface-spread VSG showed values of surface pressure which were always higher than those for VSG injected into the bulk solution. This difference, however, was no longer apparent at values of  $0.01 \text{ m}^2/\text{mg}$  and above. Due to insufficient data on VSG monolayers, further comparison with other protein monolayers is difficult. Nevertheless, the assumption made by some investigators that the interaction of protein with a lipid monolayer is inhibited when the surface pressure reaches the same value as the collapse point for the protein monolayer (Morse & Deamer, 1973) needs to be re-examined because protein at the interface loses most of its secondary and tertiary structure (Malcolm, 1973; MacRitchie, 1978). As a consequence, the number of exposed

hydrophobic side chains at the interface is not necessarily the same with protein alone and with lipid present.

Although the conformation adopted by proteins in mixed lipid monolayers is in general not known, evidence from the recombination of DMPC and DPPC vesicles with the glycoprotein, apo C-III at 23° and 41° respectively indicates that the protein undergoes a sharp increase in helicity in the presence of these lipids (Pownall *et al.*, 1977).

#### 5.54 The ratio of hydrophobic to charged amino acids

Capaldi & Vanderzooi (1972) suggested that there is a relationship between the surface activity of a protein and its amino acid composition. The hydrophobicity of proteins could be categorized by consideration of the ratios of hydrophobic to charged amino acid residues on the one hand and the surface activity associated with their strong reversible self-association. Williams (1979) used the ratio of hydrophobic to charged amino acid to examine factors affecting the ability to maintain the folding of a protein in solution. He observed that proteins with a high ratio of hydrophobic to charged amino acids constitute a group of proteins which can fold without the addition of co-factors such as calcium ions or haem. The globular proteins, for example, pig elastase, papain and lysozyme (human) fall in this group.

A second intermediate group is made up of two classes of proteins, the first of which comprises those proteins built up in segments. In these one part of the amino acid sequence has a large number of charged amino acid residues whilst the other portion is quite different. Their hydrophobic moiety can fold, leaving a long and more random external segment. The folded part may be an enzyme. This type of structure has been observed in soya-bean lipoxygenase (Egmond & Williams, 1978). The second class in this group includes those proteins,